



Analysis of forced convection of Phan–Thien–Tanner fluid in slits and tubes of constant wall temperature with viscous dissipation

S. Z. Daghighi¹ · M. Norouzi¹

Received: 25 March 2019 / Accepted: 1 October 2019 / Published online: 10 October 2019
© The Brazilian Society of Mechanical Sciences and Engineering 2019

Abstract

In the present work, analytical solutions are presented for thermal convection of the linear Phan–Thien–Tanner fluid (LPTT) in slits and tubes of constant wall temperature by taking account of the viscous dissipation term. Unlike the similar previous studies in which the advection term was neglected in the heat transfer equation, it is considered in this investigation. A continuous relation between the Nusselt number and the Brinkman number is obtained. Expressions for the temperature distribution are derived in closed form and in terms of a Frobenius series for the slit and tube flows, respectively. Based on these solutions, the effects of fluid elasticity and Brinkman number on thermal convection of LPTT fluid flows are studied in detail. It is shown that at negative Brinkman numbers (fluid cooling), increasing the Deborah number leads to a decrease in the Nusselt number, but an increase in the centerline temperature. Nonetheless, this trend is opposite for positive Brinkman numbers (fluid heating), i.e., an increase in the Nusselt number and a decrease in the centerline temperature. Also, there is a Brinkman number beyond which the Nusselt number is smaller than zero, meaning that there is weak heat convection in the flow. Also, the results confirm that the extensibility parameter affects the temperature profile in the same way as the Deborah number.

Keywords Viscoelastic fluid · Phan–Thien–Tanner model · Forced convection · Constant wall temperature tube and slit · Viscous dissipation

List of symbols

A	Area of cross section, m^2
Br	Brinkman number, $Br = \eta U^2 / k(\tilde{T}_w - \tilde{T}_m)$
c_p	Specific heat, $J\ kg^{-1}\ K^{-1}$
d_h	Hydraulic diameter, $d_h = 2R$ for tube flow and $d_h = 4H$ for slit flow, m
\mathbf{D}	Deformation rate tensor, Eq. (8)
De	Deborah number, defined as $De = \lambda U / R$ for tube case and $De = \lambda U / H$ for slit case
F	Dimensionless function
h	Heat transfer coefficient, $W\ m^{-2}\ K^{-1}$
H	Half of the distance between two parallel plates, m
J	Equals 0 for slit and 1 for tube
k	Conductivity coefficient, $W\ m^{-1}\ K^{-1}$
K	Equals 1.5 and 2 for slit and tube, respectively

Nu	Nusselt number, $Nu = hd_h/k$
p	Pressure, Pa
P	Perimeter of cross section, m
R	Tube radius, m
T	Fluid temperature, K
u	Axial velocity, ms^{-1}
U	Mean velocity, ms^{-1}
\mathbf{V}	Velocity vector
y	Radial (tube) or transverse (slit) direction, m
z	Axial direction, m

Greek symbols

α	Equals 1 for pure entropy elasticity and 0 for pure energy elasticity
α_1	$\alpha_1 = 1.5U_N/U$ for slit and $\alpha_1 = 2U_N/U$ for tube
δ	Constant, Eq. (12)
ε	Extensibility coefficient
η	Constant viscosity coefficient, Pa s
λ	Relaxation time, s
ϱ	Density, $Kg\ m^{-3}$
τ	Upper-convected derivative of stress tensor, Eq. (9)
ϕ	Viscous dissipation, Eq. (15)

Technical Editor: Daniel Onofre de Almeida Cruz, D.Sc.

✉ S. Z. Daghighi
zia.daghighi1988@gmail.com

¹ Department of Mechanical Engineering, Shahrood University of Technology, Shahrood, Iran

Subscripts

m	Mean value
max	Maximum value
N	Newtonian case
w	Wall

Superscripts

T	Transpose operator
~	Dimensional parameter

1 Introduction

It is crucial to understand clearly the physics of heat transfer in non-Newtonian flows because it affects the quality of products in polymer processing industries.

Forced heat convection of non-Newtonian fluids in ducts has been increasingly investigated. Some authors [1–9] have studied heat transfer of fluids through ducts by neglecting the viscous dissipation effect. One of the earliest studies of viscoelastic fluid flow obeying the Phan–Thien–Tanner (PTT) model was conducted by Oliveira and Pinho [10]. They presented hydrodynamic solutions to the problem of fully developed laminar flow of the PTT model through channels and pipes. Their results revealed that by increasing the dimensionless Deborah number, the velocity profiles were blunt in the center of the geometries. Pinho and Oliveira [11] investigated heat transfer of fully developed LPTT fluid in pipes and channels whose walls had a constant heat flux. They derived exact formulae for the temperature distribution in the presence of the viscous dissipation term. They reported that the heat transfer enhances by increasing either the Deborah number or the extensibility parameter. The problem of fully developed forced convection of the simplified PTT fluid in ducts with a constant wall temperature was analyzed semi-analytically by Coelho et al. [12]. In fact, they considered two cases in their study. The first case was the equilibrium between the axial convection and the radial conduction of thermal energy transfer equation, while the second case referred to the equilibrium between the radial conduction and the viscous dissipation terms. In the former case, $Br = 0$, their results showed that the Nusselt number increased monotonically when the fluid elasticity increased in the range of $0.001 \leq \epsilon We^2 \leq 100$. They also showed that for all nonzero values of the Brinkman number, the Nusselt number increased with the fluid elasticity. Pinho and Coelho [13] studied the problem of fully developed heat transfer of the SPTT fluid flow with viscous dissipation in annuli of wall subjected to either a constant wall heat flux or a constant wall temperature. They showed that for the case of constant wall heat flux, the fluid elasticity would increase the heat transfer, especially by viscous dissipation effect. Nonetheless, for the constant wall temperature

boundary condition, at low amounts of the Brinkman number, the fluid elasticity decreases the heat transfer. Norouzi [14] studied a similar problem for forced convection of PTT fluids through isothermal pipes, without the viscous dissipation effect, and derived exact solutions for the temperature distribution. Anand [15] investigated the heat transfer and entropy generation characteristics of a viscoelastic fluid flow modeled by the exponential formulation of LPTT model. By presenting an analytical model, Matias et al. [16] investigated the influence of Joule heating on the slip velocity of viscoelastic fluids.

Khan et al. [17] studied numerically the bioconvection Carreau nanofluid flow over a paraboloid surface of revolution to calculate the results of generalized Fick's and Fourier's laws on nanoscale. Arif et al. [18] studied the application of generalized Fourier heat conduction law on viscoelastic fluid flow over stretching surface. To investigate the behavior of transformed internal energy in a magnetohydrodynamic Maxwell nanofluid flow, Khan et al. [19] conducted a theoretical study. Exploring the temperature-dependent viscosity of Maxwell fluid flow, Khan et al. [20] concluded that some parameters such as the thermal stratification one control the temperature distributions inside a stretching surface. The problem of impact of generalized heat and mass flux models on Darcy–Forchheimer Williamson nanofluid flow has been recently worked out by Salahuddin et al. [21]. In their investigation, the viscosity was assumed a dependent function of temperature, and they explicated the effectiveness of some parameters like the Reynolds number and Prandtl number on dimensionless velocity and temperature profiles. Khan et al. [22] studied the effect of Darcy–Forchheimer on magnetohydrodynamic Carreau–Yasuda nanofluid flow. Their results showed that the Weissenberg number led to deceleration of the tangential and radial velocities, while the power law index accelerated them. Tanveer and Salahuddin [23] classified the simultaneous significances of complaint walls and emission of electromagnetic waves from walls which conduct Eyring–Powell fluid. They reported various solutions for dimensionless temperature distributions and velocity. Homogeneous–heterogeneous reaction effects in the flow of tangent hyperbolic fluid on a stretching cylinder were studied by Salahuddin et al. [24]. The variable fluid properties of a second-grade fluid by taking account of two different temperature-dependent viscosity models were investigated by Salahuddin et al. [25]. In their work, they derived the Nusselt number as well as the skin friction in the vicinity of a sheet surface. Haider et al. [26] analyzed the characteristics of Darcy–Forchheimer second-grade fluid flow surrounded by a deformable sheet by taking account of both variable thermal conductivity and magnetohydrodynamics.

Cruz et al. [27] presented analytical solutions for fully developed pipe and channel flows containing a Newtonian solvent described by the PTT or the finitely extensible nonlinear

elastic followed by the Peterlin approximation (FENE-P) model. Norouzi et al. [28] investigated the heat transfer characteristics for a FENE-P fluid flow through straight ducts. Also, the effect of the viscous dissipation on the thermal entrance region of non-laminar, non-Newtonian fluids is studied by some authors [29, 30]. By considering the viscous dissipation, Oliveira et al. [31] studied the Graetz problem for the FENE-P fluid in a pipe and a channel. Their investigation showed that the viscous dissipation tends to lower the Nusselt number, while the elasticity increases it.

The viscous dissipation appeared in the energy equation has an effective role in heat transfer characteristics. The present study aims to examine the LPTT viscoelastic fluid flowing through constant wall temperature slits and tubes by taking account of the viscous dissipation effect. The temperature distribution is derived as a closed-form function for the slit flow and a Frobenius series for the tube flow. In addition, the effects of the Brinkman number (both positive and negative values) and the fluid elasticity on heat transfer characteristics are discussed in detail.

As mentioned earlier, Coelho et al. [12] investigated forced convection of the LPTT fluid for two cases. But, they neglected the axial convection (advection) term for the case in which the viscous dissipation term was involved. Consequently, their result in terms of the variation of the Nusselt number via the fluid elasticity is different compared to that of the present study. Actually, the present work could be considered as the generalization of solution of Coelho et al. [12] via considering the axial convection into the heat transfer equation.

2 Governing equations and formulation

In continuum mechanics, the principles of mass conservation, momentum conservation and energy conservation must be obeyed. The continuity and the momentum equations are presented in Eqs. (1) and (2) from literature [32]

$$\tilde{\nabla} \cdot \tilde{\mathbf{V}} = 0 \tag{1}$$

$$\rho \tilde{\mathbf{V}} \cdot \tilde{\nabla} \tilde{\mathbf{V}} = -\tilde{\nabla} \tilde{p} + \tilde{\nabla} \cdot \tilde{\boldsymbol{\tau}} \tag{2}$$

where $\tilde{\mathbf{V}}$ is the velocity vector, \tilde{p} is the pressure which is supposed to be a linear function, ρ is the density and $\tilde{\boldsymbol{\tau}}$ is the stress tensor. The constitutive equation applied here for the PTT fluid [33] can be written as Eq. (3) in which f is the dimensionless function, λ is the relaxation time, η is the constant viscosity coefficient, $\tilde{\mathbf{D}}$ represents the deformation rate tensor ($\tilde{\mathbf{D}} = (\tilde{\nabla} \tilde{\mathbf{V}} + \tilde{\nabla} \tilde{\mathbf{V}}^T)/2$) and $\tilde{\boldsymbol{\tau}}$ indicates the Oldroyd's upper-convected derivative of the stress tensor shown in Eq. (4):

$$f(tr(\tilde{\boldsymbol{\tau}}))\tilde{\boldsymbol{\tau}} + \lambda \overset{\nabla}{\tilde{\boldsymbol{\tau}}} = 2\eta\tilde{\mathbf{D}} \tag{3}$$

$$\overset{\nabla}{\tilde{\boldsymbol{\tau}}} = \frac{D\tilde{\boldsymbol{\tau}}}{Dt} - (\tilde{\nabla}\tilde{\mathbf{V}}^T \cdot \tilde{\boldsymbol{\tau}} + \tilde{\boldsymbol{\tau}} \cdot \tilde{\nabla}\tilde{\mathbf{V}}) \tag{4}$$

Since there is no exact solution for the exponential type of the PTT fluid, just the linear form of the PTT fluid is adopted here in, and the corresponding dimensionless function will be

$$f(tr(\tilde{\boldsymbol{\tau}})) = 1 + \frac{\epsilon\lambda}{\eta} tr(\tilde{\boldsymbol{\tau}}) \tag{5}$$

where ϵ is the fluid extensibility coefficient limiting the fluid extensional viscosity. Indeed, nonzero values of ϵ preclude the possibility of infinite extensional viscosity in a stretching flow in contrast to the upper-convected Maxwell (UCM) model possessing $\epsilon = 0$.

The underlying assumptions for the present study are summarized as follows. The model parameters are independent of temperature, the flow is incompressible, rectilinear, laminar and hydrodynamically and thermally fully developed, and the viscoelastic fluid is simulated with the LPTT constitutive equation in two dimensions. Since the flow is hydrodynamically fully developed, the velocity profile (along the longitudinal axis) is only dependent on the vertical side, and since the flow is thermally fully developed, the axial conduction is negligible relative to the radial conduction [32].

After some mathematical simplifications, the two following equations are derived from Eqs. (3) and (4) which are applicable for both the tube and slit flows.

$$tr(\tilde{\boldsymbol{\tau}}) = \tilde{\tau}_{yy} = \frac{2\lambda\tilde{\tau}_{yz}^2}{\eta} \tag{6}$$

$$\frac{d\tilde{u}_z}{d\tilde{y}} = f\left(\frac{2\lambda\tilde{\tau}_{yz}^2}{\eta}\right) \frac{\tilde{\tau}_{yz}}{\eta} \tag{7}$$

Consequently, by considering the linear form of the PTT model, as shown in Eq. (5), the transverse (slit case) or radial (tube case) velocity gradient will be expressed as

$$\frac{d\tilde{u}_z}{d\tilde{y}} = \left[1 + \frac{2\epsilon\lambda^2\tilde{\tau}_{yz}^2}{\eta^2}\right] \frac{\tilde{\tau}_{yz}}{\eta} \tag{8}$$

Finally, with the help of the momentum equation given in Eq. (2) and considering the component in the axial direction, we have,

$$\tilde{\tau}_{yz} = \frac{d\tilde{p}}{d\tilde{z}} \frac{\tilde{y}}{(1+j)} \tag{9}$$

where j equals 0 for the slit flow and 1 for the tube flow and $d\tilde{p}/d\tilde{z}$ is the pressure gradient. Also, \tilde{y} is radial or transverse coordinate depending on the use of radial or Cartesian coordinate. By integrating Eq. (8) from an arbitrary position in the radial or transverse coordinate to the wall, and replacing the axial component of the stress tensor, in turn, the velocity distribution will be derived as [10]:

$$\frac{\tilde{u}(y)}{U} = K \frac{U_N}{U} (1 - y^2) \left(1 + 4K^2 \epsilon De^2 \left(\frac{U_N}{U} \right)^2 (1 + y^2) \right) \tag{10}$$

where \tilde{u} is the main flow velocity (axial velocity), U is the mean velocity defined as the volumetric flow rate divided by the cross-sectional area, K takes the respective values of 1.5 and 2 for the slit and the tube flows and U_N is the corresponding mean velocity for the Newtonian flow which is $U_N = -d\tilde{p}/d\tilde{z}(R^2/8\eta)$ for the tube flow and $U_N = -d\tilde{p}/d\tilde{z}(H^2/3\eta)$ for the slit flow. In addition, y is the dimensionless variable defined as $y = \tilde{y}/R$ for the tube flow and $y = \tilde{y}/H$ for the slit flow (here H is half of width of the slit). The dimensionless Deborah number is defined as $De = \lambda U/R$ for the tube flow and $De = \lambda U/H$ for the slit flow and represents the level of the fluid elasticity. Expectedly, for $De = 0$ or $\epsilon = 0$, Eq. (10) reduces to the parabolic profile with a maximum velocity at the centerline equal to K . Oliveira and Pinho [10] showed that the velocity ratio (U_N/U) can be calculated from the following formulation in terms of the rheological properties:

$$\frac{U_N}{U} = \frac{432^{1/6}(\delta^{2/3} - 2^{2/3})}{6b^{1/2}\delta^{1/3}} \tag{11}$$

where δ is:

$$\delta = (4 + 27b)^{1/2} + 3^{3/2}b^{1/2} \tag{12}$$

In Eqs. (11) and (12), b is a constant, $b = 54/5(\epsilon De^2)$ for the slit flow and $b = 64/3(\epsilon De^2)$ for the tube flow. Now we turn into the energy equation which plays a crucial role in the present study.

The energy equation should be treated cautiously. For viscoelastic materials, as Peters and Baijens [34] reported in their work, the mechanical energy is partly dissipated and partly stored as elastic energy. They presented the general energy equation in the form of Eq. (13).

$$\rho c_p \dot{\hat{T}} = \nabla \cdot (k \nabla \hat{T}) + \alpha \tilde{\tau} : \tilde{D} + (1 - \alpha) \frac{tr(\tilde{\tau})}{2\lambda} \left(1 + \frac{\epsilon \lambda}{\eta} tr(\tilde{\tau}) \right) \tag{13}$$

where c_p is the specific heat, \hat{T} is the temperature material derivative, k is the thermal conductivity, $\tau : D$ is the viscous dissipation which is a contribution of the entropy elasticity

and therefore contributes to temperature change. The last term in Eq. (13) denotes the energy elasticity representing the energy stored elastically and does not relate to temperature variation. The split of the mechanical energy into the entropic elasticity and the energy elasticity is measured by α . In the case of pure entropy elasticity we have $\alpha = 1$, while in pure elastic energy it is $\alpha = 0$.

In light of the assumptions mentioned earlier and by considering an isotropic thermal conductivity, Eq. (13) can be simplified for both the tube and the slit cases as follows:

$$\rho c_p \tilde{u}_z \frac{\partial \hat{T}}{\partial \tilde{z}} = k \left(\frac{\partial^2 \hat{T}}{\partial \tilde{y}^2} + \frac{j}{\tilde{y}} \frac{\partial \hat{T}}{\partial \tilde{y}} \right) + \alpha \tilde{\phi} + (1 - \alpha) \frac{\tilde{\tau}_{yy}}{2\lambda} \left(1 + \frac{\epsilon \lambda}{\eta} \tilde{\tau}_{yy} \right) \tag{14}$$

As it is available in the literature [32], for $Pe_D \gg 1$ the axial conduction is neglected in comparison with the radial conduction. Also, by considering the hypothesis of a fully developed flow in the axial direction where the velocity component is zero, the transverse convection term of the energy equation is neglected. In addition, the viscous dissipation term $\tilde{\tau} : \tilde{D}$ is replaced by $\tilde{\phi}$ and is resulted by tensor product of the velocity gradient into the stress tensor which for the present problem will be reduced to $\tilde{\phi} = \tilde{\tau}_{yz} d\tilde{u}_z/d\tilde{y}$, and after replacing the velocity gradient by Eq. (8), the dimensional viscous dissipation will be

$$\tilde{\phi} = \left(1 + \frac{2\epsilon \lambda^2 \tilde{\tau}_{yz}^2}{\eta^2} \right) \frac{\tilde{\tau}_{yz}^2}{\eta} \tag{15}$$

It is worthwhile to mention that the viscous dissipation term is not the same for the tube and the slit cases since they have a different shear stress ($\tilde{\tau}_{yz}$) as presented in Eq. (9). After some mathematical simplifications, the final energy equation will be derived as

$$\tilde{u}_z \frac{\partial \hat{T}}{\partial \tilde{z}} = \frac{k}{\rho c_p} \left(\frac{\partial^2 \hat{T}}{\partial \tilde{y}^2} + \frac{j}{\tilde{y}} \frac{\partial \hat{T}}{\partial \tilde{y}} \right) + \frac{1}{\rho c_p} \left(1 + \frac{2\epsilon \lambda^2 \tilde{\tau}_{yz}^2}{\eta^2} \right) \frac{\tilde{\tau}_{yz}^2}{\eta} \tag{16}$$

As it can be seen from the above equation, the term α has been diminished. Indeed, the terms involving α cancel out and interestingly the final result, as shown in Eq. (16), is mathematically equivalent to setting $\alpha = 1$ in Eq. (14). In order to render the variables dimensionless, the following expressions are introduced.

$$u = \frac{\tilde{u}}{U}, \quad T = \frac{\hat{T} - \hat{T}_w}{\hat{T}_m - \hat{T}_w} \quad \left\{ \begin{array}{l} \text{For slit flow: } z = \frac{\tilde{z}}{H}, \quad y = \frac{\tilde{y}}{H} \quad \text{and} \quad \phi = \frac{\tilde{\phi}}{3\eta U^2/H^2} \\ \text{For tube flow: } z = \frac{\tilde{z}}{R}, \quad y = \frac{\tilde{y}}{R} \quad \text{and} \quad \phi = \frac{\tilde{\phi}}{4\eta U^2/R^2} \end{array} \right. \tag{17}$$

where \tilde{T}_w is the wall temperature and \tilde{T}_m denotes the fluid mean temperature in the tube or the slit across the longitudinal coordinate. Consequently, the dimensionless form of the viscous dissipation term (Eq. (15)) will be

$$\phi = (3 + j)(U_N/U)^2 y^2 (1 + 2\alpha_2 y^2) \tag{18}$$

in which we have $\alpha_2 = 9\epsilon De^2 (U_N/U)^2$ for the slit flow and $\alpha_2 = 16\epsilon De^2 (U_N/U)^2$ for the tube flow. It is easily provable that the viscous dissipation term for $De = 0$, the Newtonian fluid, is $\phi = (3 + j)y^2$.

Now it aims to derive a relationship for the dimensional axial gradient of temperature ($\partial\tilde{T}/\partial\tilde{z}$). In this regard, it is known that in the fully developed thermal condition, the axial gradient of the dimensionless temperature is zero [35]:

$$\frac{\partial T}{\partial z} = \frac{\partial}{\partial z} \left(\frac{\tilde{T} - \tilde{T}_w}{\tilde{T}_m - \tilde{T}_w} \right) = 0 \tag{19}$$

By expanding the above equation and knowing that the tube wall temperature is constant, we have:

$$\frac{\partial \tilde{T}}{\partial \tilde{z}} = T \frac{d\tilde{T}_m}{d\tilde{z}} \tag{20}$$

In addition, the dimensional axial gradient of the mean temperature appeared in the above equation, $d\tilde{T}_m/d\tilde{z}$, could be obtained by considering a balance of energy on a differential control volume and taking account of the viscous dissipation for both the cases as follows:

$$\rho \tilde{A} U c_p d\tilde{T}_m = h(\tilde{T}_w - \tilde{T}_m) \tilde{P} d\tilde{z} + \int_{\tilde{V}} \left(1 + \frac{2\epsilon\lambda^2}{\eta^2} \tilde{\tau}_{yz}^2 \right) \frac{\tilde{\tau}_{yz}^2}{\eta} d\tilde{A} d\tilde{z}$$

$$\left\{ \begin{array}{l} \text{For slit flow: } \frac{d\tilde{T}_m}{d\tilde{z}} = \frac{h(\tilde{T}_w - \tilde{T}_m)}{\rho H U c_p} + \frac{3\eta U^2 (U_N/U)^2 (1 + b(U_N/U)^2)}{\rho H^2 U c_p} \\ \text{For tube flow: } \frac{d\tilde{T}_m}{d\tilde{z}} = \frac{2h(\tilde{T}_w - \tilde{T}_m)}{\rho R U c_p} + \frac{8\eta U^2 (U_N/U)^2 (1 + b(U_N/U)^2)}{\rho R^2 U c_p} \end{array} \right. \tag{21}$$

where \tilde{P} and \tilde{A} are the perimeter and the area of the cross section, respectively. By applying Eq. (22) which is reported by Oliveira and Pinho [10], on Eq. (21), finally the axial gradient of the mean temperature can be expressed in the form of Eq. (23).

$$\frac{U_N}{U} \left(1 + b \left(\frac{U_N}{U} \right)^2 \right) = 1 \tag{22}$$

$$\left\{ \begin{array}{l} \text{For slit flow: } \frac{d\tilde{T}_m}{d\tilde{z}} = \frac{h(\tilde{T}_w - \tilde{T}_m)}{\rho H U c_p} + \frac{3\eta U_N}{\rho H^2 c_p} \\ \text{For tube flow: } \frac{d\tilde{T}_m}{d\tilde{z}} = \frac{2h(\tilde{T}_w - \tilde{T}_m)}{\rho R U c_p} + \frac{8\eta U_N}{\rho R^2 c_p} \end{array} \right. \tag{23}$$

Finally, the dimensionless form of the energy equation for the LPTT flow in slits and tubes of constant wall temperature is derived as

$$\frac{d^2 T}{dy^2} + \frac{j}{y} \frac{dT}{dy} + \alpha_1 (1 - y^2) (1 + \alpha_2 (1 + y^2)) \left(\frac{1}{4 - 3j} \text{Nu} + 2(j + 1)\alpha_1 \text{Br} \right) T - 4\alpha_1^2 \text{Br} (1 + 2\alpha_2 y^2) y^2 = 0 \tag{24}$$

where we have $\alpha_1 = 1.5 U_N/U$ and $\alpha_1 = 2 U_N/U$ for the slit and tube flows, respectively. Moreover, there are two well-known dimensionless numbers, namely the Nusselt number and the Brinkman number, which are defined as $\text{Nu} = h d_h/k$ and $\text{Br} = \eta U^2 / (k(\tilde{T}_w - \tilde{T}_m))$, respectively. The parameter h is the convective heat transfer coefficient and d_h is the hydraulic diameter ($d_h = 2R$ for the tube flow and $d_h = 4H$ for the slit flow).

3 Analytical solution

As mentioned before, the motive of the present study is to obtain the dimensionless temperature field, $T(y)$, in constant wall temperature slits and tubes. To this aim, the temperature distribution is determined by solving the second-order

non-homogeneous differential equation [Eq. (24)] by applying an analytical method. Besides, there are two boundary conditions consisting of the symmetry condition at the centerline [Eq. (25)] and the constant wall temperature [Eq. (26)]. Since the number of unknown parameters exceeds the number of the boundary conditions, a physical constrain will be introduced for each case [Eqs. (29) and (32)].

$$\text{at } y = 0 \Rightarrow \frac{dT}{dy} = 0 \tag{25}$$

$$\text{at } y = 1 \Rightarrow T = 0 \tag{26}$$

3.1 Slit flow

By substituting $j=0$ into Eq. (24) and then solving it, the temperature distribution for the LPTT fluid flow in a slit of constant wall temperature will be determined as follows:

$$\begin{aligned}
 &T(y) \\
 &= C_1 \text{HeunT} \left(\begin{array}{l} 0.13 \frac{\alpha_1^2 (8\alpha_1 \text{Br} + \text{Nu})^2 (2\alpha_2 + 1)^2}{(\alpha_1 \alpha_2 (8\alpha_1 \text{Br} + \text{Nu}))^{4/3}}, 0, \\ 0.7211 \frac{\alpha_1 (8\alpha_1 \text{Br} + \text{Nu})}{(\alpha_1 \alpha_2 (8\alpha_1 \text{Br} + \text{Nu}))^{2/3}}, -0.6934 \sqrt[6]{\alpha_1 \alpha_2 (8\alpha_1 \text{Br} + \text{Nu})} y \end{array} \right) \\
 &\times e^{\frac{1}{12} \frac{\alpha_1 (8\alpha_1 \text{Br} + \text{Nu}) (2\alpha_2 y^2 + 3)}{\sqrt{\alpha_1 \alpha_2 (8\alpha_1 \text{Br} + \text{Nu})}}} \\
 &+ C_2 \text{HeunT} \left(\begin{array}{l} 0.13 \frac{\alpha_1^2 (8\alpha_1 \text{Br} + \text{Nu})^2 (2\alpha_2 + 1)^2}{(\alpha_1 \alpha_2 (8\alpha_1 \text{Br} + \text{Nu}))^{4/3}}, 0, \\ 0.7211 \frac{\alpha_1 (8\alpha_1 \text{Br} + \text{Nu})}{(\alpha_1 \alpha_2 (8\alpha_1 \text{Br} + \text{Nu}))^{2/3}}, 0.6934 \sqrt[6]{\alpha_1 \alpha_2 (8\alpha_1 \text{Br} + \text{Nu})} y \end{array} \right) \\
 &\times e^{-\frac{1}{12} \frac{\alpha_1 (8\alpha_1 \text{Br} + \text{Nu}) (2\alpha_2 y^2 + 3)}{\sqrt{\alpha_1 \alpha_2 (8\alpha_1 \text{Br} + \text{Nu})}}} \\
 &+ \left[\begin{array}{l} \text{HeunT} \left(\begin{array}{l} 0.13 \frac{\alpha_1 (8B\alpha_1 + \text{Nu}) (2\alpha_2 + 1)^2}{\alpha_2^3 \sqrt{\alpha_1 \alpha_2 (8B\alpha_1 + \text{Nu})}}, 0, 0.7211 \frac{\alpha_1 (8B\alpha_1 + \text{Nu})}{(\alpha_1 \alpha_2 (8B\alpha_1 + \text{Nu}))^{2/3}}, \\ -0.6934 \sqrt[6]{\alpha_1 \alpha_2 (8B\alpha_1 + \text{Nu})} y \end{array} \right) \\ e^{\frac{1}{12} \frac{(2y^3 \alpha_2 + 3y) \sqrt{\alpha_1 \alpha_2 (8B\alpha_1 + \text{Nu})}}{\alpha_2}} \int \frac{A}{B} dy \\ - \text{HeunT} \left(\begin{array}{l} 0.13 \frac{\alpha_1 (8B\alpha_1 + \text{Nu}) (2\alpha_2 + 1)^2}{\alpha_2^3 \sqrt{\alpha_1 \alpha_2 (8B\alpha_1 + \text{Nu})}}, 0, 0.7211 \frac{\alpha_1 (8B\alpha_1 + \text{Nu})}{(\alpha_1 \alpha_2 (8B\alpha_1 + \text{Nu}))^{2/3}}, \\ 0.6934 \sqrt[6]{\alpha_1 \alpha_2 (8B\alpha_1 + \text{Nu})} y \end{array} \right) \\ e^{-\frac{1}{6} \frac{y \sqrt{\alpha_1 \alpha_2 (8B\alpha_1 + \text{Nu})} (\alpha_2 y^2 + \frac{3}{2})}{\alpha_2}} \int \frac{C}{B} dy \end{array} \right] \\
 &\times 24\alpha_1^2 \text{Br} \sqrt{\alpha_1 \alpha_2 (8\alpha_1 \text{Br} + \text{Nu})}
 \end{aligned} \tag{27}$$

where A , B and C are:

$$\begin{aligned}
 A &= (2y^4\alpha_2 + y^2)e^{-\frac{1}{6} \frac{y\sqrt{\alpha_1\alpha_2(8B\alpha_1 + Nu)}(\alpha_2 y^2 + \frac{3}{2})}{\alpha_2}} \\
 &\times \text{HeunT} \left(\begin{array}{l} 0.13 \frac{(\alpha_1\alpha_2(8B\alpha_1 + Nu))^{2/3}(2\alpha_2 + 1)^2}{\alpha_2^2}, 0, 0.7211 \frac{\alpha_1(8B\alpha_1 + Nu)}{(\alpha_1\alpha_2(8B\alpha_1 + Nu))^{2/3}}, \\ 0.6934\sqrt[6]{\alpha_1\alpha_2(8B\alpha_1 + Nu)}y \end{array} \right) \\
 B &= \left(\begin{array}{l} 48 \left(B\alpha_1 + \frac{Nu}{8} \right) \left(\alpha_2 y^2 + \frac{1}{2} \right) \alpha_1 \\ \text{HeunT} \left(\begin{array}{l} 0.13 \frac{\alpha_1(8B\alpha_1 + Nu)(2\alpha_2 + 1)^2}{\alpha_2^3\sqrt{\alpha_1\alpha_2(8B\alpha_1 + Nu)}}, 0, 0.7211 \frac{\alpha_1(8B\alpha_1 + Nu)}{(\alpha_1\alpha_2(8B\alpha_1 + Nu))^{2/3}}, \\ 0.6934\sqrt[6]{\alpha_1\alpha_2(8B\alpha_1 + Nu)}y \end{array} \right) \\ - 4.16(\alpha_1\alpha_2(8B\alpha_1 + Nu))^{2/3} \\ \text{HeunTPrime} \left(\begin{array}{l} 0.13 \frac{\alpha_1(8B\alpha_1 + Nu)(2\alpha_2 + 1)^2}{\alpha_2^3\sqrt{\alpha_1\alpha_2(8B\alpha_1 + Nu)}}, 0, 0.7211 \frac{\alpha_1(8B\alpha_1 + Nu)}{(\alpha_1\alpha_2(8B\alpha_1 + Nu))^{2/3}}, \\ 0.6934\sqrt[6]{\alpha_1\alpha_2(8B\alpha_1 + Nu)}y \end{array} \right) \\ \times \text{HeunT} \left(\begin{array}{l} 0.13 \frac{\alpha_1(8B\alpha_1 + Nu)(2\alpha_2 + 1)^2}{\alpha_2^3\sqrt{\alpha_1\alpha_2(8B\alpha_1 + Nu)}}, 0, 0.7211 \frac{\alpha_1(8B\alpha_1 + Nu)}{(\alpha_1\alpha_2(8B\alpha_1 + Nu))^{2/3}}, \\ - 0.6934\sqrt[6]{\alpha_1\alpha_2(8B\alpha_1 + Nu)}y \end{array} \right) \\ - 4.16(\alpha_1\alpha_2(8B\alpha_1 + Nu))^{2/3} \\ \times \text{HeunTPrime} \left(\begin{array}{l} 0.13 \frac{\alpha_1(8B\alpha_1 + Nu)(2\alpha_2 + 1)^2}{\alpha_2^3\sqrt{\alpha_1\alpha_2(8B\alpha_1 + Nu)}}, 0, 0.7211 \frac{\alpha_1(8B\alpha_1 + Nu)}{(\alpha_1\alpha_2(8B\alpha_1 + Nu))^{2/3}}, \\ - 0.6934\sqrt[6]{\alpha_1\alpha_2(8B\alpha_1 + Nu)}y \end{array} \right) \\ \times \text{HeunT} \left(\begin{array}{l} 0.13 \frac{\alpha_1(8B\alpha_1 + Nu)(2\alpha_2 + 1)^2}{\alpha_2^3\sqrt{\alpha_1\alpha_2(8B\alpha_1 + Nu)}}, 0, 0.7211 \frac{\alpha_1(8B\alpha_1 + Nu)}{(\alpha_1\alpha_2(8B\alpha_1 + Nu))^{2/3}}, \\ 0.6934\sqrt[6]{\alpha_1\alpha_2(8B\alpha_1 + Nu)}y \end{array} \right) \end{array} \right) \tag{28} \\
 C &= (2y^4\alpha_2 + y^2)e^{\frac{1}{12} \frac{(2y^3\alpha_2 + 3y)\sqrt{\alpha_1\alpha_2(8B\alpha_1 + Nu)}}{\alpha_2}} \\
 &\times \text{HeunT} \left(\begin{array}{l} 0.13 \frac{(\alpha_1\alpha_2(8B\alpha_1 + Nu))^{2/3}(2\alpha_2 + 1)^2}{\alpha_2^2}, 0, 0.7211 \frac{\alpha_1(8B\alpha_1 + Nu)}{(\alpha_1\alpha_2(8B\alpha_1 + Nu))^{2/3}}, \\ - 0.6934\sqrt[6]{\alpha_1\alpha_2(8B\alpha_1 + Nu)}y \end{array} \right)
 \end{aligned}$$

As it can be seen, Eq. (27) represents a closed-form solution containing a special mathematical function, HeunT, for the slit case. Regarding Eq. (27), there are three unknown constant parameters in the slit temperature distribution, namely C_1 , C_2 and Nu which one of them, C_1 , vanishes by applying Eq. (26) to Eq. (27). Unfortunately, there are no analytical solutions for the two integral expressions in Eq. (27). Therefore, these integrals have been solved numerically using the 1/3 Simpson rule. Because of the

number of the unknown parameters, a physical constrain is presented in Eq. (29) which is the product of the dimensionless velocity profile into the dimensionless temperature distribution throughout the area of the geometry.

$$\int_0^1 u(y)T(y)dy = 1 \tag{29}$$

Then, with applying Eqs. (25) and (29) to Eq. (27), a linear system of two equations with two variables (C_2 and Nu) will appear by solving it; the slit temperature distribution will be completely determined.

3.2 Tube flow

The solution of forced heat convection of the LPTT fluid flow in a constant wall temperature tube can be obtained by

solving Eq. (24) for $j = 1$. There is no closed-form solution for this case, and therefore, the temperature distribution has been solved by the Frobenius method. The corresponding temperature distribution for the tube flow is presented in Eq. (30).

$$\begin{aligned}
 T(y) = C_1 & \left(\begin{aligned} & \left(1 - \frac{1}{4} \alpha_1 (Nu(1 + \alpha_2) + 4k_1(1 + \alpha_2)Br)y^2 \right. \\ & \left. + \frac{1}{64} \alpha_1 \left(\begin{aligned} & Nu(\alpha_1 Nu(1 + \alpha_2)^2 + 4) \\ & + 8(\alpha_1^2 Nu(1 + \alpha_2)^2 + 2\alpha_1 + 2\alpha_1^3(1 + \alpha_2)^2 Br) Br \end{aligned} \right) \right) y^4 \\ & - \frac{1}{2304} \alpha_1 (4\alpha_1 Br + Nu) \\ & \times \left(\begin{aligned} & \left(\alpha_1 Nu(\alpha_1 Nu(1 + \alpha_2)^3 + 20(1 + \alpha_2)) - 64\alpha_2 + \right. \\ & \left. 8 \left(\begin{aligned} & \alpha_1^3 Nu(1 + \alpha_2)^3 + 10\alpha_1^2(1 + \alpha_2) + \right. \\ & \left. 2\alpha_1^4(1 + \alpha_2)^3 Br \end{aligned} \right) Br \end{aligned} \right) y^6 + O(y^7) \end{aligned} \right) \\
 & \ln(y) \left(\begin{aligned} & \left(1 - \frac{1}{4} \alpha_1 (Nu(1 + \alpha_2) + 4\alpha_1(1 + \alpha_2)Br)y^2 \right. \\ & \left. + \frac{1}{64} \alpha_1 \left(\begin{aligned} & Nu(\alpha_1 Nu(1 + \alpha_2)^2 + 4) + \right. \\ & \left. 8(\alpha_1^2 Nu(1 + \alpha_2)^2 + 2\alpha_1 + 2\alpha_1^3(1 + \alpha_2)^2 Br) Br \end{aligned} \right) \right) y^4 \\ & - \frac{1}{2304} \alpha_1 (4\alpha_1 Br + Nu) \\ & \times \left(\begin{aligned} & \left(\alpha_1 Nu(\alpha_1 Nu(1 + \alpha_2)^3 + 20(1 + \alpha_2)) - 64\alpha_2 + \right. \\ & \left. 8 \left(\begin{aligned} & \alpha_1^3 Nu(1 + \alpha_2)^3 + 10\alpha_1^2(1 + \alpha_2) + \right. \\ & \left. 2\alpha_1^4(1 + \alpha_2)^3 Br \end{aligned} \right) Br \end{aligned} \right) y^6 + O(y^7) \end{aligned} \right) \\
 & + \frac{1}{4} \alpha_1 (Nu(1 + \alpha_2) + 4\alpha_1(1 + \alpha_2)Br)y^2 \\
 & + C_2 \left(\begin{aligned} & \left(\frac{1}{16} \alpha_1 (Nu + 4\alpha_1 Br) \right. \\ & \left. - \frac{3}{128} \alpha_1 \left(\begin{aligned} & \alpha_1 Nu^2(1 + \alpha_2)^2 + 4Nu \\ & + 8(\alpha_1^2 Nu(1 + \alpha_2)^2 + 2\alpha_1 + 2Br\alpha_1^3(1 + \alpha_2)^2) Br \end{aligned} \right) \right) y^4 \\ & - \frac{3}{576} (Nu + 4\alpha_1 Br)\alpha_1 \\ & \times (\alpha_1 Nu(1 + \alpha_2) - 8\alpha_2 + 4\alpha_1^2(1 + \alpha_2)Br) \\ & + \frac{11}{13824} (Nu + 4\alpha_1 Br)\alpha_1 \\ & \times \left(\begin{aligned} & \alpha_1^2 Nu^2(1 + \alpha_2)^3 + 20Nu\alpha_1(1 + \alpha_2) - 64\alpha_2 \\ & 8 \left(\begin{aligned} & \alpha_1^3 Nu(1 + \alpha_2)^3 + 10\alpha_1^2(1 + \alpha_2) + \right. \\ & \left. 2\alpha_1^4(1 + \alpha_2)^3 Br \end{aligned} \right) Br \end{aligned} \right) y^6 + O(y^7) \\
 & + Br \left(\frac{1}{4} \alpha_1^2 y^4 + \left(\frac{2}{9} \alpha_1^2 \alpha_2 - \frac{1}{144} \alpha_1^2 (\alpha_1 Nu(1 + \alpha_2) + 4\alpha_1^2(1 + 4\alpha_2)Br) \right) y^6 \right) + O(y^7)
 \end{aligned} \right) \tag{30}
 \end{aligned}$$

By applying the boundary condition given in Eq. (25) to Eq. (30) and considering the singularity of Eq. (30) at $y=0$, the constant C_2 vanishes. Suffice it to say that the temperature distribution is finite throughout the cross section. Finally, the temperature distribution, up to eight-order terms, for the tube flow is presented in Eq. (31) in which C_1 is replaced by the maximum temperature located at the center of the tube.

4 Results and discussion

In this section, the results of forced convective heat transfer of the linear PTT fluid with viscous dissipation through constant wall temperature slits and tubes are discussed in detail. This study aims to clarify the effects of fluid elasticity ($0.1 \leq De \leq 100$), extensibility ($1 \leq \epsilon \leq 10$) and the

$$T(y) = T_c \left(\begin{aligned} & \left(1 - \frac{1}{4}\alpha_1(\text{Nu}(1 + \alpha_2) + 4k_1(1 + \alpha_2)\text{Br})y^2 \right. \\ & \left. + \frac{1}{64}\alpha_1 \left(\text{Nu}(\alpha_1\text{Nu}(1 + \alpha_2)^2 + 4) \right. \right. \\ & \left. \left. + 8(\alpha_1^2\text{Nu}(1 + \alpha_2)^2 + 2\alpha_1 + 2\alpha_1^3(1 + \alpha_2)^2\text{Br})\text{Br} \right) y^4 \right. \\ & \left. - \frac{1}{2304}(\text{Nu} + 4\alpha_1\text{Br})\alpha_1 \right. \\ & \left. \times \left(\alpha_1\text{Nu}(\alpha_1\text{Nu}(1 + \alpha_2)^3 + 20(1 + \alpha_2)) - 64\alpha_2 \right) \right. \\ & \left. + 8 \left(\alpha_1^3\text{Nu}(1 + \alpha_2)^3 + 10\alpha_1^2(1 + \alpha_2) + \right. \right. \\ & \left. \left. 2\alpha_1^4(1 + \alpha_2)^3\text{Br} \right) \text{Br} \right) y^6 \\ & + \frac{1}{147456}(\text{Nu} + 4\alpha_1\text{Br})\alpha_1^2 \\ & \left(\alpha_1^2\text{Nu}^3(1 + \alpha_2)^4 + 56\alpha_1\text{Nu}^2(1 + \alpha_2)^2 \right. \\ & \left. - 640\alpha_2\text{Nu}(1 + \alpha_2) + 144\text{Nu} \right. \\ & \left. \times \left(\left(12\alpha_1^3\text{Nu}^2(1 + \alpha_2)^4\text{Br} + 48\alpha_1^4\text{Nu}(1 + \alpha_2)^4\text{Br} + \right. \right. \right. \\ & \left. \left. \left. + 64\alpha_1^5(1 + \alpha_2)^4\text{Br}^2 + 448\alpha_1^2\text{Nu}(1 + \alpha_2)^2 - \right. \right. \right. \\ & \left. \left. \left. 2560\alpha_1\alpha_2(1 + \alpha_2) + 576\alpha_1 + 896\alpha_1^3(1 + \alpha_2)^2\text{Br} \right) \text{Br} \right) y^8 \right) \\ & + \text{Br} \left(\frac{1}{4}\alpha_1^2y^4 + \left(\frac{2}{9}\alpha_2 - \frac{1}{144}\alpha_1(1 + \alpha_2)(\text{Nu} + 4\alpha_1\text{Br}) \right) \alpha_1^2y^6 \right. \\ & \left. + \left(\frac{1}{256} - \frac{1 + \alpha_2}{2304} \left(8\alpha_2 - \frac{1}{4}\alpha_1(1 + \alpha_2)(\text{Nu} + 4\alpha_1\text{Br}) \right) \right) \alpha_1^3(\text{Nu} + 4\alpha_1\text{Br})y^8 \right) + \dots \end{aligned} \right) \tag{31}$$

Like the slit case, the Nusselt number and the maximum temperature have been calculated using the boundary condition shown in Eq. (26) as well as the physical constrain presented in Eq. (32).

$$\int_0^1 u(y)T(y)dy = \frac{1}{2} \tag{32}$$

Brinkman number ($-10 \leq \text{Br} \leq 10$) on the heat transfer characteristics in a fully developed regime. The results for the tube flow are presented and discussed in detail, while those relating to the slit flow are summarized in tabular form (for the similarity). For estimating the dimensionless parameters that appear in this study, the typical values [36] of physical parameters are listed in Table 1. Also, the reliability of the present results is gained for the Newtonian fluid in tubes and slits in Sect. 4.1.

4.1 Validation

The authors believe that the existing studies on forced convection of the LPTT fluid flow do not match the present work and cannot be used for validation. The present results have been therefore validated only in the Newtonian case ($De = 0$ and $\epsilon = 0$) with those available in the literature. In the present work, the Nusselt number for a constant wall temperature tube flow has been calculated as $Nu = 3.6571$ which closely matches the value of $Nu = 3.66$ [32, 37]. For the slit case, the Nusselt number in a constant wall temperature slit is $Nu = 7.541$ [32], and this investigation revealed the value of $Nu = 7.5407$. It can be concluded that the present results are in good correspondence with those available in the literature. In Sect. 4.2, the effects of either negative or positive Brinkman numbers as well as the fluid elasticity on the heat transfer characteristics are examined.

4.2 Effects of Brinkman number and fluid elasticity

Figure 1 demonstrates the effect of negative Brinkman numbers, namely $Br = -10, -1$ and -0.1 , on the dimensionless temperature, considering different values of the extensibility parameter (ϵ) and the Deborah number (De). By considering the definition of the Brinkman number, given by $Br = \eta U^2 / k(\tilde{T}_w - \tilde{T}_m)$, at negative Brinkman numbers there is fluid cooling adjacent to the wall. Figure 1 shows that at fixed values of ϵ and De , by increasing the Brinkman number, the flow temperature and its temperature gradient in the vicinity of the wall fall, leading to a smaller Nusselt number. As demonstrated in Fig. 1, at $De = 0.1$ when Br increases from $Br = -10$ to $Br = -0.1$, the respective Nusselt numbers decrease dramatically from $Nu = 38.4616$ to $Nu = 4.1799$. Indeed, higher values of Br strengthen the cooling process in the wall area, where the viscous dissipation effect is the strongest. Following a diametrically opposed trend, the centerline temperature, T_c , increases by Br and the temperature profiles in the vicinity of the core region displace upward in the radial direction. According to Fig. 1, by increasing De

Table 1 Typical values of physical and geometrical parameters used for estimating the dimensionless parameters in the present study

Parameter	Value	Unit
Br	$\frac{\eta U^2}{k(T_w - T_m)} = \frac{9.245(0.2054)^2}{0.1067(210 - 200)} = 0.3655$	-
c_p	840	J kg ⁻¹ K ⁻¹
De	$\lambda U / H = 0.0018(0.2054) / 0.0125 = 0.0296$	-
h	$\frac{Nu k}{d_h} = \begin{cases} (1.7028)(0.1067) / 0.025 = 7.2675 \text{ tube} \\ (4.9363)(0.1067) / 0.05 = 10.5341 \text{ slit} \end{cases}$	W m ⁻² K ⁻¹
H	0.0125	m
k	$k_0(k_0^* + k_s^* T)$ $= 0.08(0.7753 + 0.00118(273.15 + 200))$ $= 0.1067$	W m ⁻¹ K ⁻¹
Nu	$\begin{cases} 1.7065 \text{ tube} \\ 4.9363 \text{ slit} \end{cases}$	-
R	0.0125	m
U	$\frac{Re \eta}{\rho D} = \frac{0.5(9.245)}{900(0.025)} = 0.2054$	ms ⁻¹
ϵ	0.1	-
η	$\eta_0 a_T$ $= 10 \left\{ \exp \left[\alpha \left(\frac{1}{T_m + 273.15} - \frac{1}{T_0 + 273.15} \right) \right] \right\}$ $= 10 \left\{ \exp \left[1720 \left(\frac{1}{200 + 273.15} - \frac{1}{190 + 273.15} \right) \right] \right\}$ $= 9.245$	Pa s
λ	$\lambda_0 a_T$ $= 0.002 \left\{ \exp \left[\alpha \left(\frac{1}{T + 273.15} - \frac{1}{T_0 + 273.15} \right) \right] \right\}$ $= 0.002 \left\{ \exp \left[1720 \left(\frac{1}{200 + 273.15} - \frac{1}{190 + 273.15} \right) \right] \right\}$ $= 0.0018$	s
ρ	900	kg m ⁻³

the Nusselt number decreases and the centerline temperature increases. Consequently, the Deborah number intensifies the effect of the Brinkman number, meaning that the higher the Deborah number, the higher the Brinkman number, leading to lower Nusselt numbers, but higher centerline temperatures. Moreover, the increasing De causes a wider blunt velocity distribution in the core region as well as a lower value of centerline velocity, leading to weaker heat convection in the vicinity of the core. This is why the lowest value of the centerline temperature is recorded for $De = 0.1$, and the centerline temperature increases as De increases. Regarding the rheological aspect, when De increases the fluid shear-thinning behavior intensifies which results in a better heat distribution in the flow as shown in Fig. 1. Furthermore, as

Br increases, the effect of De seems to be lessened. In other words, when the Brinkman number increases from $Br = -10$ to $Br = -0.1$, the deviation between the three temperature profiles nearly vanishes (for either the Nusselt number or the centerline temperature). For instance, at $Br = -10$ we have $Nu = 38.4616$ at $De = 0.1$ and $Nu = 5.1371$ at $De = 100$, while the corresponding values at $Br = -0.1$ are nearly the same, $Nu = 4.1799$ and $Nu = 4.1760$, respectively. And the same goes for the centerline temperature values.

Figure 1 also depicts the effect of the fluid extensibility parameter on the temperature distribution. It is found that at a certain Brinkman number, ϵ decreases the wall temperature gradient and therefore Nu , but it also increases the centerline temperature which is apparent by considering Fig. 1b.

Fig. 1 Dimensionless temperature distribution for negative Brinkman numbers in constant wall temperature tubes **a** $\epsilon = 1$ and **b** $\epsilon = 10$

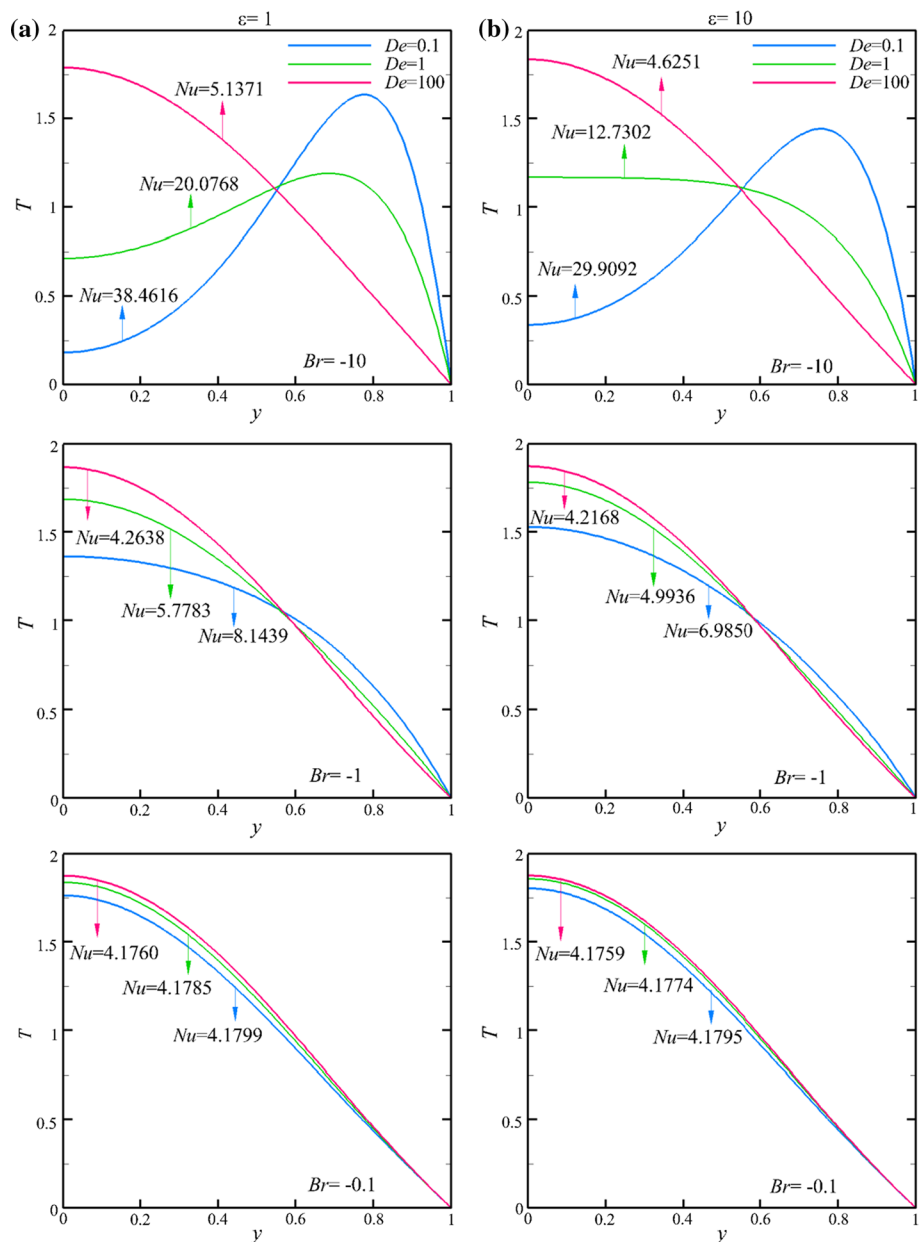
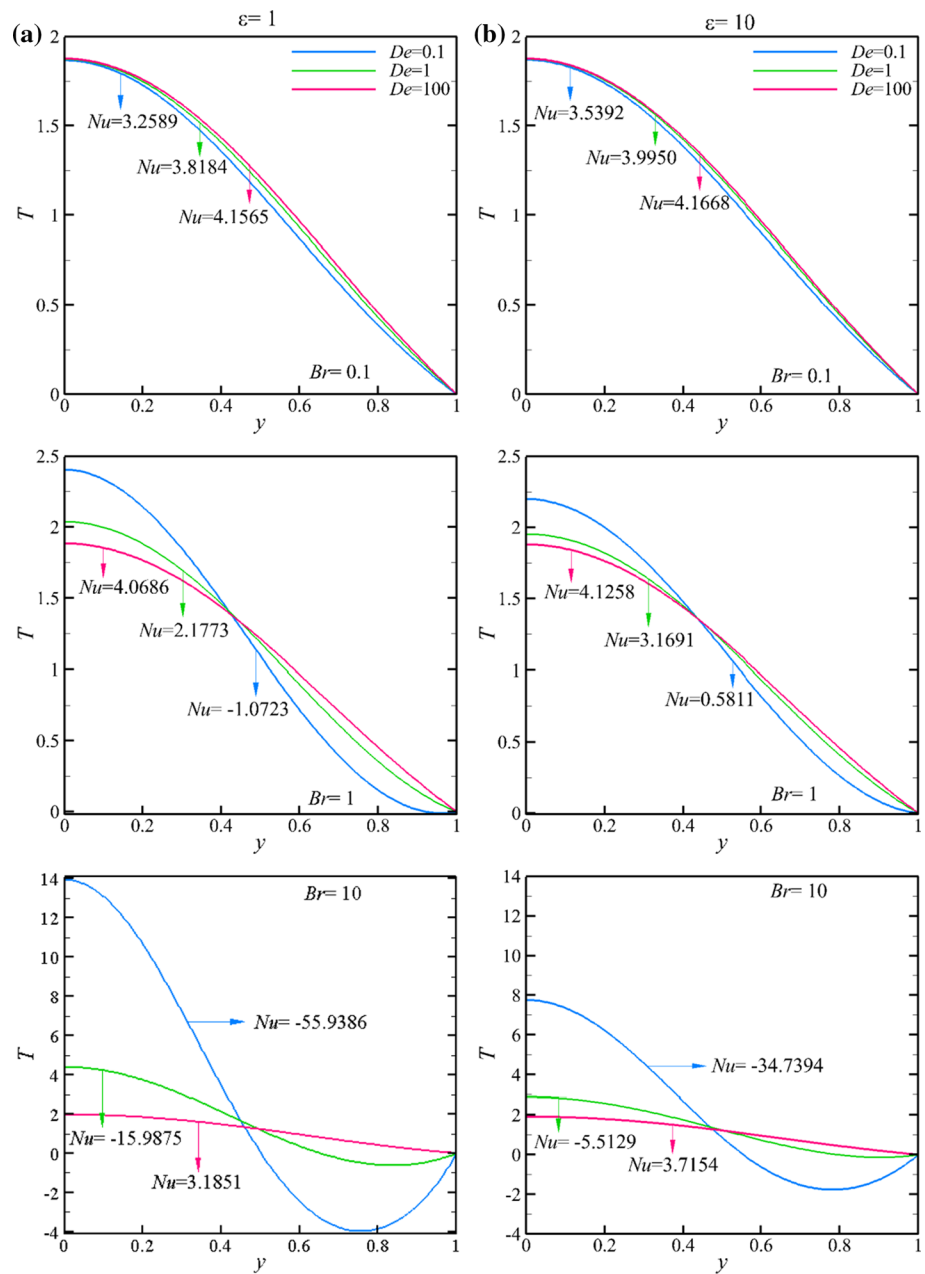


Fig. 2 Dimensionless temperature distribution for positive Brinkman numbers in constant wall temperature tubes **a** $\varepsilon = 1$ and **b** $\varepsilon = 10$



Indeed, the extensibility parameter affects the temperature profile in the same way as the Deborah number. For example, at $Br = -10$ and $De = 0.1$ as demonstrated in Fig. 1b the Nusselt number is equal to $Nu = 38.4616$ at $\varepsilon = 1$, while it is decreased to $Nu = 29.9092$ at $\varepsilon = 10$.

Similarly, Fig. 2 illustrates the effects of positive Brinkman numbers on temperature distribution in the LPTT fluid. It is worthwhile mentioning that, as a fact, the Nusselt number decreases continuously with the Brinkman number and

thus it has lower values at positive Brinkman numbers. Generally, nearly all the trends presented at positive Brinkman numbers are opposite to those shown at negative Brinkman numbers. When the Brinkman number is greater than zero, flow is supposed to be heated, since the wall temperature is larger than the mean temperature. But it is revealed that at $Br = 0.1$ the flow is cooled further. Such small positive values of Br behave in the same way as $Br = 0$ does. At these values, the dominance of viscous dissipation is not

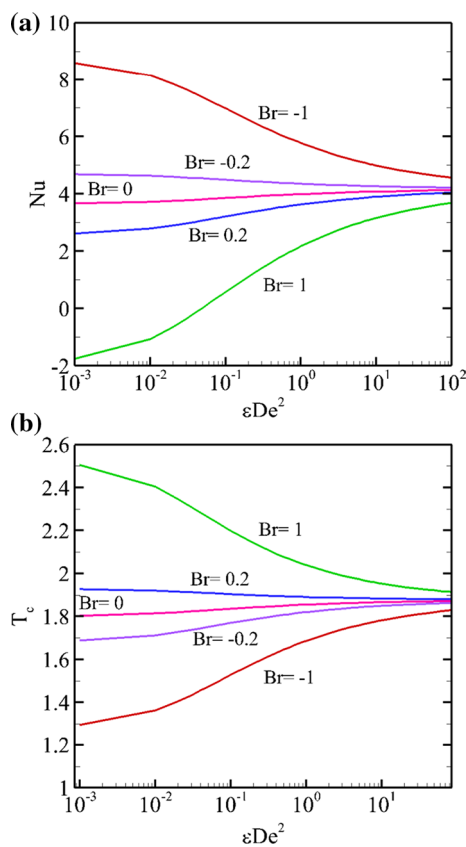


Fig. 3 Variations of **a** Nusselt number and **b** centerline temperature with fluid elasticity ϵDe^2 for different Brinkman numbers in tube flow

strong enough to overcome fluid cooling, and therefore, the fluid in the vicinity of the wall becomes colder. As shown in Fig. 2, at $Br = 0.1$ and $\epsilon = 1$, when $De = 0.1$, the fluid is cooled down and there is a negative temperature gradient next to the wall. When the Deborah number increases from $De = 0.1$ to $De = 100$, because of an improvement in the fluid shear-thinning behavior, both the Nusselt number and centerline temperature increase, and the temperature profiles move upward entirely. As Br increases, the viscous dissipation effect will be stronger and much more energy will be produced in the flow. As depicted in Fig. 2, for the case $Br = 1$, the viscous dissipation effect overcomes the cooling effect and the Nusselt number decreases to a negative number at $De = 0.1$. Indeed, at this moment there is the heating process in the flow which is borne out with the positive wall temperature gradient, leading to a negative Nusselt number ($Nu = -1.0723$). In this condition and at a constant Brinkman number, when the Deborah number increases, because of a larger value of velocity adjacent to the wall, the flow

becomes warm faster than other areas, augmenting the heating process. As a consequence, the temperature profile in the vicinity of the wall moves upward which causes the temperature gradient to be positive, thereby resulting in a positive Nusselt number as well ($Nu = 4.0686$ at $De = 100$). Like the cooling process, when De increases, the centerline velocity becomes lower, weakening the heat convection in the core region. For this reason, at higher De the centerline temperature follows a downward trend. In the following, through further growth in the Brinkman number up to $Br = 10$, a dramatic fall has been observed in the value of Nu , implying too weak heat convection in the flow ($Nu = -55.9386$). At this moment, the strength of the viscous dissipation is so much that causes difficulty in proper distribution of the heat generated as it can be seen in the case of $De = 0.1$. Since a huge amount of energy is accumulated next to the wall, where the viscous dissipation effect is the highest, the heat convection is too weak which causes the flow temperature to remain negative at radial distances more than $y \approx 5$. Conversely, the flow temperature in the core region is by far higher than other areas ($T_c \approx 14$). Again, by increasing De there will be better heat distribution throughout the flow and at $De = 100$ it is much better where the temperature profile varies steadily in the radial coordinate ($Nu = 3.1851$). In fluid heating, at higher Deborah numbers the value of the centerline temperature falls ($T_c \approx 2$), so the flow in the core region will be heated slightly which is attributed to a lower centerline velocity.

As mentioned earlier, the extensibility parameter only intensifies the Deborah number effect. In comparison with Fig. 2a, the temperature profiles in Fig. 2b become closer to each other and there will be a lower deviation between them, leading to better heat distribution.

Figure 3a, b shows the impact of the fluid elasticity shown by ϵDe^2 on the heat transfer characteristics. As explained before, it is clear from the line graphs that for the cases in which $Br = 0.2$ and $Br = 1$ there is fluid heating in the flow, while other cases are related to the cooling process.

According to the Fig. 3a, the Nusselt number depends heavily on the Brinkman number and it increases by decreasing the Brinkman number from positive to negative values.

Figures 4, 5 and 6 show the slit case which shows similar results in comparison with the tube case.

In "Appendix," the results of the Nusselt number and the centerline temperature are reported (Tables 2, 3, 4, 5, 6, 7, 8, 9) for both the tube and slit flows for various values of the Brinkman number, Deborah number and the extensibility parameter.

Fig. 4 Dimensionless temperature distribution for negative Brinkman numbers in constant wall temperature slits **a** $\varepsilon = 1$ and **b** $\varepsilon = 10$

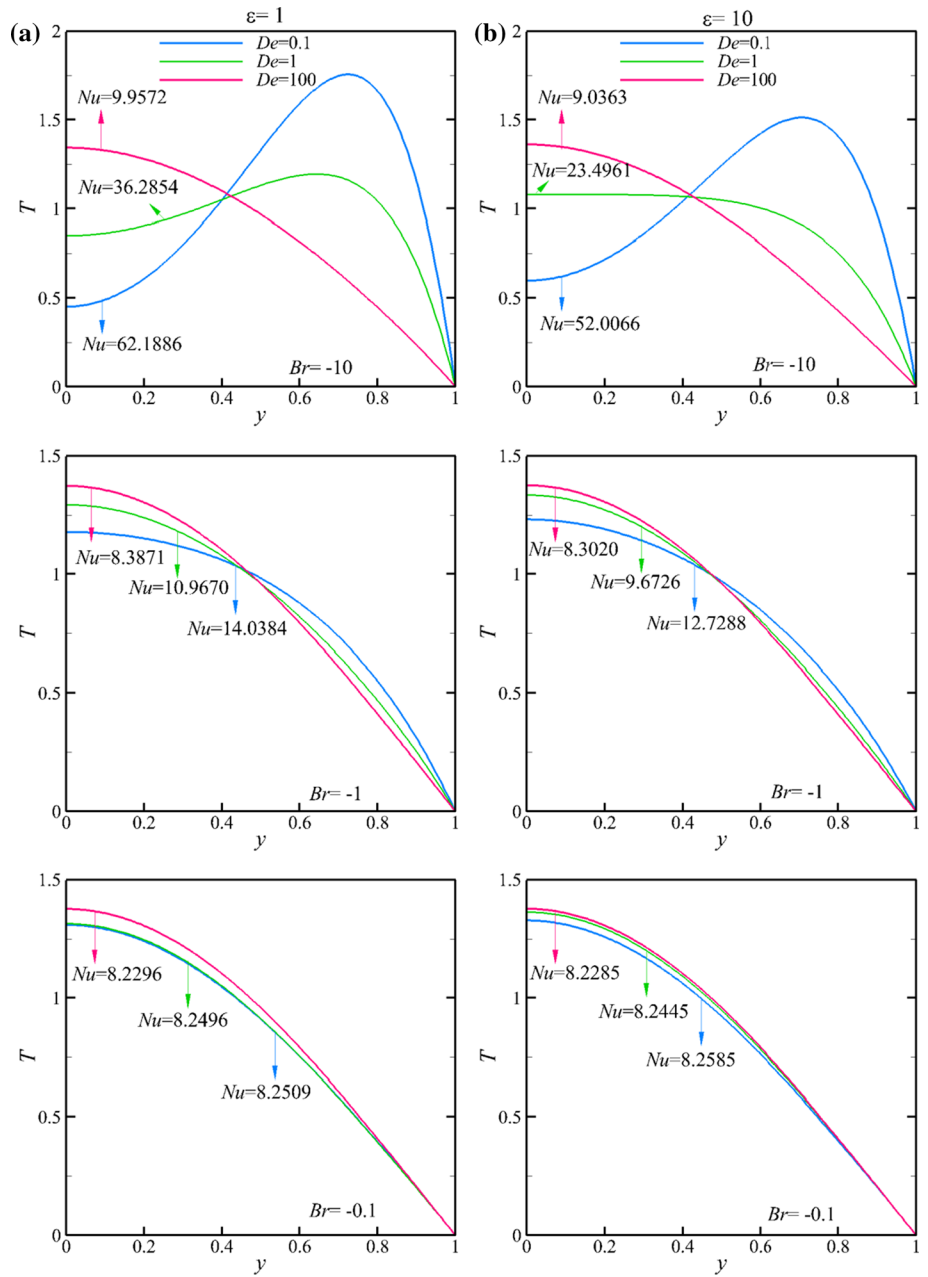
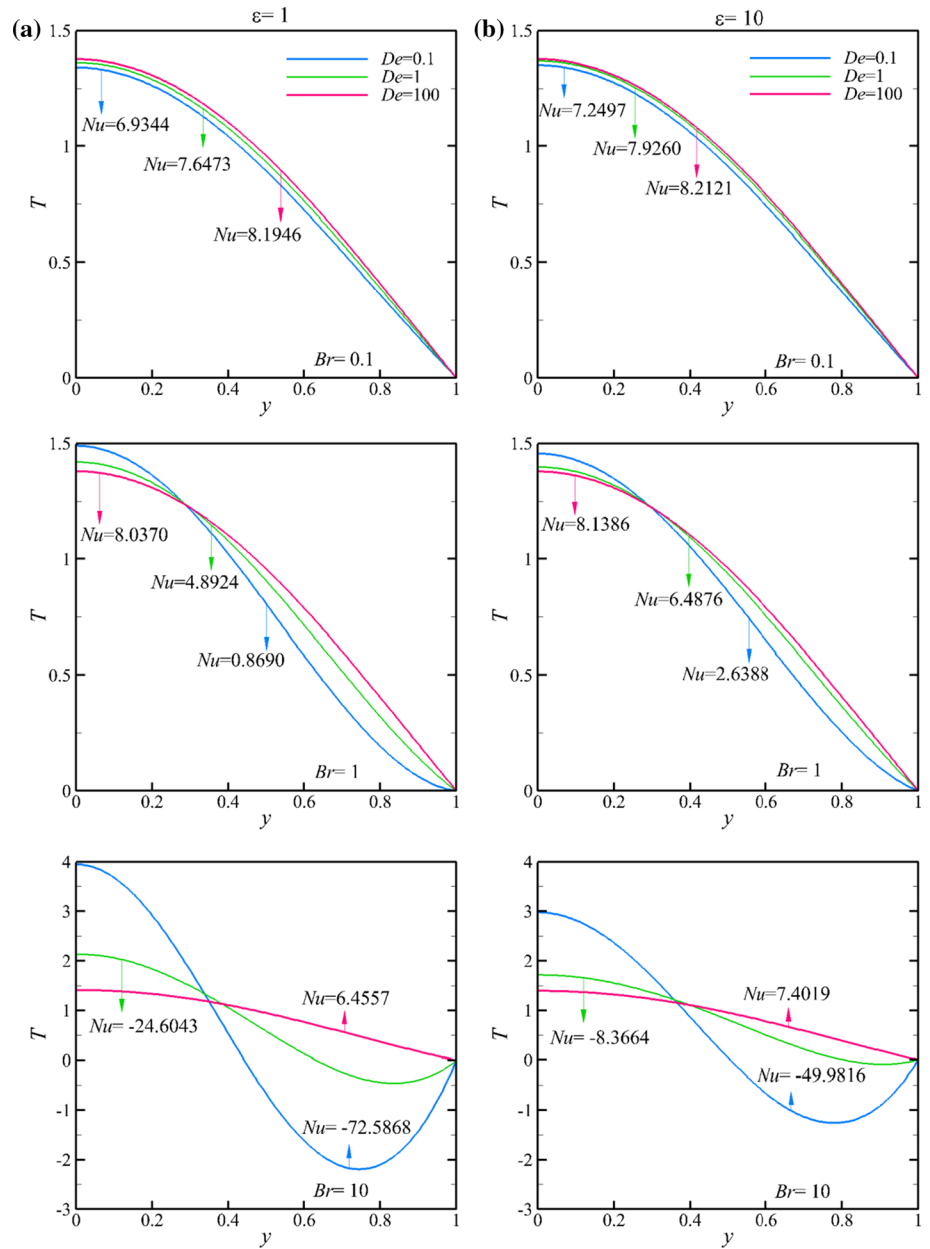


Fig. 5 Dimensionless temperature distribution for positive Brinkman numbers in constant wall temperature slits **a** $\varepsilon = 1$ and **b** $\varepsilon = 10$



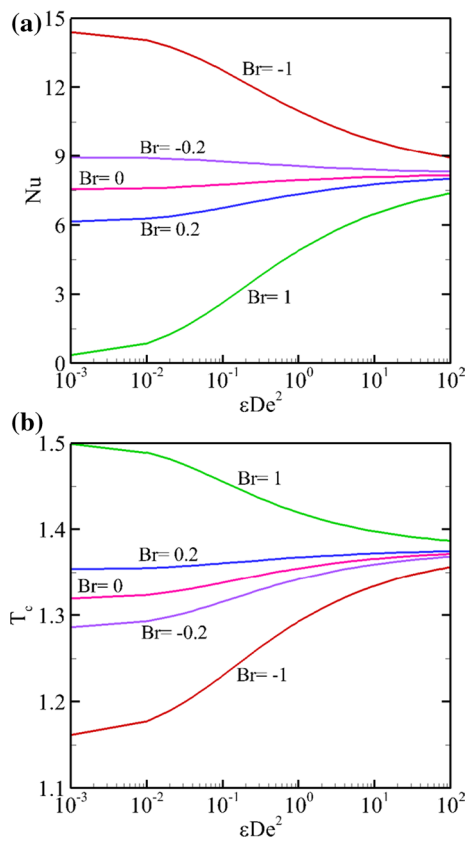


Fig. 6 Variations of **a** Nusselt number and **b** centerline temperature with fluid elasticity ϵDe^2 for different Brinkman numbers in slit flow

5 Conclusions

In this article, exact analytical solutions for heat convection in the simplified PTT fluid flow through tubes and slits whose walls are subjected to a constant temperature have

been presented for the first time. The viscous dissipation term is taken into account. Expressions for the temperature distribution are derived in closed form for the slit case and in terms of a Frobenius series for the tube case. It is shown that the Nusselt number is heavily dependent on the Brinkman number and decreases continuously with the Brinkman number. The results revealed that the variations in the cooling and heating processes are inverted. In the cooling process, the Nusselt number decreases when the Deborah number and the extensibility parameter increase, while the centerline temperature increases. However, during the heating process the Nusselt number increases and the centerline temperature decreases. In addition, they vary in two completely different trends when the Deborah number and the Brinkman number increase.

Compliance with ethical standards

Conflict of interest The authors declare that they have no conflict of interest.

Appendix: Tube and slit Nusselt number and centerline temperature

For the sake of conciseness, the Nusselt number and centerline temperature data for both the tube and slit cases are given in Tables 2, 3, 4, 5, 6, 7, 8 and 9. Results have been calculated for $Br = -10, -1, -0.1, 0, 0.1, 1, 10$, for three scores of the extensibility parameters $\epsilon = 1, \sqrt{10}$ and 10 and for a range of Deborah numbers $0.1 \leq De \leq 100$.

Table 2 Nusselt number and centerline temperature values for the LPTT fluid flow in a constant wall temperature tube for negative Brinkman numbers at different values of extensibility parameter and Deborah number

De	Br = -10		Br = -1		Br = -0.1		Br = 0	
	Nu	T_c	Nu	T_c	Nu	T_c	Nu	T_c
$\epsilon = 1$								
0.1	38.4616	0.1822	8.1439	1.3624	4.1799	1.7628	3.7213	1.8139
1	20.0768	0.7145	5.7783	1.6869	4.1785	1.8379	3.9986	1.8554
10	8.4332	1.5037	4.5723	1.8315	4.1766	1.8675	4.1326	1.8715
20	6.9181	1.6319	4.4291	1.8478	4.1764	1.8707	4.1482	1.8732
30	6.2873	1.6867	4.3702	1.8544	4.1762	1.8719	4.1546	1.8739
40	5.9276	1.7183	4.3368	1.8582	4.1761	1.8727	4.1583	1.8743
50	5.6904	1.7394	4.3148	1.8606	4.1761	1.8731	4.1607	1.8745
60	5.5202	1.7545	4.2991	1.8624	4.1761	1.8735	4.1624	1.8747
70	5.3910	1.7660	4.2872	1.8637	4.1760	1.8737	4.1637	1.8749
80	5.2891	1.7752	4.2778	1.8648	4.1760	1.8739	4.1647	1.8750
90	5.2061	1.7826	4.2701	1.8656	4.1760	1.8741	4.1655	1.8751
100	5.1371	1.7888	4.2638	1.8663	4.1760	1.8742	4.1662	1.8751
$\epsilon = \sqrt{10}$								
0.1	34.6784	0.2359	7.6291	1.4381	4.1798	1.7815	3.7838	1.8242
1	15.9939	0.9487	5.3311	1.7421	4.1779	1.8495	4.0488	1.8618
10	7.1325	1.6134	4.4492	1.8455	4.1764	1.8702	4.1460	1.8730
20	6.0667	1.7061	4.3497	1.8567	4.1762	1.8724	4.1569	1.8741
30	5.6276	1.7449	4.3090	1.8613	4.1761	1.8733	4.1613	1.8746
40	5.3783	1.7672	4.2860	1.8639	4.1760	1.8738	4.1638	1.8749
50	5.2144	1.7819	4.2709	1.8655	4.1760	1.8741	4.1654	1.8750
60	5.0970	1.7924	4.2601	1.8667	4.1760	1.8743	4.1666	1.8752
70	5.0080	1.8004	4.2519	1.8677	4.1760	1.8745	4.1675	1.8753
80	4.9378	1.8068	4.2455	1.8684	4.1759	1.8746	4.1682	1.8753
90	4.8808	1.8119	4.2402	1.8690	4.1759	1.8748	4.1688	1.8754
100	4.8334	1.8162	4.2359	1.8694	4.1759	1.8748	4.1693	1.8754
$\epsilon = 10$								
0.1	29.9092	0.3384	6.9850	1.5286	4.1795	1.8028	3.8601	1.8360
1	12.7302	1.1698	4.9936	1.7825	4.1774	1.8577	4.0862	1.8662
10	6.2165	1.6929	4.3636	1.8552	4.1762	1.8721	4.1554	1.8740
20	5.4746	1.7586	4.2949	1.8629	4.1761	1.8736	4.1628	1.8748
30	5.1711	1.7857	4.2669	1.8660	4.1760	1.8742	4.1659	1.8751
40	4.9993	1.8012	4.2511	1.8678	4.1760	1.8745	4.1676	1.8753
50	4.8865	1.8114	4.2408	1.8689	4.1759	1.8747	4.1687	1.8754
60	4.8058	1.8187	4.2334	1.8697	4.1759	1.8749	4.1695	1.8755
70	4.7448	1.8242	4.2278	1.8704	4.1759	1.8750	4.1701	1.8755
80	4.6966	1.8286	4.2233	1.8708	4.1759	1.8751	4.1706	1.8756
90	4.6576	1.8321	4.2198	1.8712	4.1759	1.8752	4.1710	1.8756
100	4.6251	1.8351	4.2168	1.8716	4.1759	1.8753	4.1713	1.8757

Table 3 Nusselt number and centerline temperature values for LPTT fluid flow in a constant wall temperature tube for positive Brinkman numbers at different values of extensibility parameter and Deborah number

De	Br = 0		Br = 0.1		Br = 1		Br = 10	
	Nu	T_c	Nu	T_c	Nu	T_c	Nu	T_c
$\varepsilon = 1$								
0.1	3.7213	1.8139	3.2589	1.8663	-1.0723	2.4046	-55.9386	13.9279
1	3.9986	1.8554	3.8184	1.8731	2.1773	2.0387	-15.9875	4.3877
10	4.1326	1.8715	4.0885	1.8756	3.6906	1.9123	-0.3830	2.3138
20	4.1482	1.8732	4.1201	1.8758	3.8665	1.8990	1.2920	2.1443
30	4.1546	1.8739	4.1331	1.8759	3.9386	1.8936	1.9715	2.0785
40	4.1583	1.8743	4.1404	1.8759	3.9795	1.8905	2.3545	2.0421
50	4.1607	1.8745	4.1452	1.8759	4.0063	1.8885	2.6053	2.0185
60	4.1624	1.8747	4.1487	1.8760	4.0255	1.8871	2.7845	2.0018
70	4.1637	1.8749	4.1513	1.8760	4.04	1.8861	2.9199	1.9893
80	4.1647	1.8750	4.1534	1.8760	4.0515	1.8852	3.0266	1.9795
90	4.1655	1.8751	4.1551	1.8760	4.0608	1.8845	3.1132	1.9715
100	4.1662	1.8751	4.1565	1.8760	4.0686	1.8840	3.1851	1.9650
$\varepsilon = \sqrt{10}$								
0.1	3.7838	1.8242	3.3852	1.8678	-0.3199	2.3050	-46.0977	10.4188
1	4.0488	1.8618	3.9194	1.8741	2.7462	1.9886	-9.8613	3.4717
10	4.1460	1.8730	4.1157	1.8757	3.8418	1.9008	1.0588	2.1673
20	4.1569	1.8741	4.1376	1.8759	3.9637	1.8917	2.2068	2.0560
30	4.1613	1.8746	4.1465	1.8759	4.0134	1.8880	2.6715	2.0124
40	4.1638	1.8749	4.1516	1.8760	4.0415	1.8859	2.9332	1.9881
50	4.1654	1.8750	4.1549	1.8760	4.0599	1.8846	3.1046	1.9723
60	4.1666	1.8752	4.1573	1.8760	4.0731	1.8836	3.2269	1.9611
70	4.1675	1.8753	4.1591	1.8760	4.0830	1.8829	3.3194	1.9527
80	4.1682	1.8753	4.1605	1.8760	4.0909	1.8823	3.3922	1.9461
90	4.1688	1.8754	4.1616	1.8760	4.0973	1.8818	3.4513	1.9408
100	4.1693	1.8754	4.1626	1.8760	4.1026	1.8815	3.5003	1.9363
$\varepsilon = 10$								
0.1	3.8601	1.8360	3.5392	1.8697	0.5811	2.1991	-34.7394	7.7604
1	4.0862	1.8662	3.9950	1.8748	3.1691	1.9534	-5.5129	2.8986
10	4.1554	1.8740	4.1345	1.8759	3.9467	1.8930	2.0471	2.0712
20	4.1628	1.8748	4.1496	1.8760	4.0306	1.8867	2.8323	1.9974
30	4.1659	1.8751	4.1558	1.8760	4.0648	1.8842	3.1498	1.9682
40	4.1676	1.8753	4.1592	1.8760	4.0840	1.8828	3.3285	1.9519
50	4.1687	1.8754	4.1615	1.8760	4.0966	1.8819	3.4454	1.9413
60	4.1695	1.8755	4.1631	1.8760	4.1057	1.8812	3.5289	1.9337
70	4.1701	1.8755	4.1644	1.8761	4.1125	1.8807	3.5919	1.9281
80	4.1706	1.8756	4.1653	1.8761	4.1178	1.8803	3.6416	1.9236
90	4.1710	1.8756	4.1661	1.8761	4.1222	1.88	3.6819	1.92
100	4.1713	1.8757	4.1668	1.8761	4.1258	1.8798	3.7154	1.9170

Table 4 Nusselt number data as a function of ϵDe^2 in a tube flow for different values of Brinkman number

ϵDe^2	Br = -1	Br = -0.2	Br = 0	Br = 0.2	Br = 1
0.001	8.5845	4.6884	3.6664	2.6245	-1.7430
0.01	8.1439	4.6348	3.7213	2.7928	-1.0723
0.02	7.8564	4.6003	3.7564	2.9003	-0.6481
0.03	7.6565	4.5764	3.7805	2.9740	-0.3591
0.04	7.5039	4.5583	3.7988	3.0298	-0.1414
0.05	7.3809	4.5438	3.8134	3.0745	0.0322
0.06	7.2783	4.5317	3.8256	3.1116	0.1760
0.07	7.1904	4.5213	3.8360	3.1433	0.2983
0.08	7.1137	4.5124	3.8450	3.1708	0.4043
0.09	7.0458	4.5044	3.8530	3.1951	0.4978
0.1	6.9850	4.4973	3.8601	3.2168	0.5811
0.2	6.5897	4.4513	3.9061	3.3566	1.1155
0.3	6.3677	4.4256	3.9316	3.4342	1.4104
0.4	6.2165	4.4082	3.9489	3.4868	1.6093
0.5	6.1034	4.3952	3.9618	3.5259	1.7570
0.6	6.0139	4.3849	3.9720	3.5568	1.8733
0.7	5.9405	4.3765	3.9803	3.5821	1.9684
0.8	5.8784	4.3694	3.9873	3.6034	2.0485
0.9	5.8250	4.3632	3.9934	3.6217	2.1173
1.0	5.7783	4.3579	3.9986	3.6377	2.1773
2.0	5.4952	4.3256	4.0304	3.7343	2.5386
3.0	5.3490	4.3089	4.0468	3.7838	2.7235
4.0	5.2538	4.2981	4.0574	3.8160	2.8435
5.0	5.1845	4.2902	4.0651	3.8394	2.9305
6.0	5.1308	4.2841	4.0710	3.8575	2.9978
7.0	5.0874	4.2791	4.0759	3.8721	3.0521
8.0	5.0512	4.2750	4.0799	3.8842	3.0973
9.0	5.0204	4.2715	4.0833	3.8946	3.1358
10.0	4.9936	4.2685	4.0862	3.9036	3.1691
20.0	4.8359	4.2506	4.1036	3.9564	3.3651
30.0	4.7572	4.2417	4.1123	3.9827	3.4626
40.0	4.7068	4.2359	4.1178	3.9996	3.5249
50.0	4.6705	4.2318	4.1218	4.0117	3.5697
60.0	4.6427	4.2287	4.1249	4.0209	3.6040
70.0	4.6203	4.2261	4.1273	4.0284	3.6316
80.0	4.6017	4.2240	4.1294	4.0346	3.6545
90.0	4.5860	4.2222	4.1311	4.0398	3.6739
100.0	4.5723	4.2207	4.1326	4.0444	3.6906

Table 5 Centerline temperature values as a function of ϵDe^2 in tube flow for different values of Brinkman number

ϵDe^2	Br = -1	Br = -0.2	Br = 0	Br = 0.2	Br = 1
0.001	1.2950	1.6885	1.8044	1.9279	2.5048
0.01	1.3624	1.7131	1.8139	1.9202	2.4046
0.02	1.4050	1.7282	1.8197	1.9157	2.3470
0.03	1.4341	1.7383	1.8236	1.9128	2.3099
0.04	1.4560	1.7459	1.8266	1.9107	2.2830
0.05	1.4735	1.7518	1.8289	1.9091	2.2621
0.06	1.4880	1.7567	1.8308	1.9077	2.2451
0.07	1.5003	1.7608	1.8324	1.9066	2.2310
0.08	1.5109	1.7644	1.8337	1.9056	2.2189
0.09	1.5203	1.7675	1.8349	1.9048	2.2083
0.1	1.5286	1.7702	1.8360	1.9040	2.1991
0.2	1.5821	1.7876	1.8428	1.8994	2.1419
0.3	1.6114	1.7970	1.8464	1.8970	2.1119
0.4	1.6311	1.8032	1.8488	1.8954	2.0923
0.5	1.6457	1.8078	1.8505	1.8942	2.0780
0.6	1.6571	1.8114	1.8519	1.8933	2.0669
0.7	1.6665	1.8143	1.8530	1.8925	2.0580
0.8	1.6743	1.8167	1.8539	1.8919	2.0506
0.9	1.6811	1.8188	1.8547	1.8913	2.0442
1.0	1.6869	1.8206	1.8554	1.8909	2.0387
2.0	1.7221	1.8312	1.8595	1.8881	2.0065
3.0	1.7399	1.8366	1.8615	1.8867	1.9905
4.0	1.7514	1.84	1.8628	1.8858	1.9804
5.0	1.7598	1.8425	1.8637	1.8852	1.9731
6.0	1.7662	1.8444	1.8645	1.8847	1.9675
7.0	1.7714	1.8460	1.8650	1.8843	1.9630
8.0	1.7757	1.8472	1.8655	1.8839	1.9593
9.0	1.7793	1.8483	1.8659	1.8837	1.9561
10.0	1.7825	1.8492	1.8662	1.8834	1.9534
20.0	1.8010	1.8546	1.8683	1.8820	1.9377
30.0	1.8102	1.8573	1.8692	1.8813	1.93
40.0	1.8160	1.8590	1.8699	1.8808	1.9251
50.0	1.8202	1.8602	1.8703	1.8805	1.9216
60.0	1.8234	1.8611	1.8707	1.8802	1.9190
70.0	1.8260	1.8619	1.8709	1.88	1.9168
80.0	1.8281	1.8625	1.8712	1.8799	1.9151
90.0	1.8299	1.8630	1.8713	1.8797	1.9136
100.0	1.8315	1.8634	1.8715	1.8796	1.9123

Table 6 Nusselt number and centerline temperature values for LPTT fluid flow in a constant wall temperature slit for negative Brinkman numbers at different values of extensibility parameter and Deborah number

De	Br = -10		Br = -1		Br = -0.1		Br = 0	
	Nu	T_c	Nu	T_c	Nu	T_c	Nu	T_c
$\varepsilon = 1$								
0.1	62.1886	0.4510	14.0384	1.1776	8.2509	1.3085	7.5941	1.3239
1	36.2854	0.8508	10.9670	1.2931	8.2496	1.3141	7.9512	1.3549
10	15.8619	1.2267	8.9392	1.3564	8.2365	1.37	8.1583	1.3716
20	13.1526	1.2795	8.6845	1.3639	8.2334	1.3726	8.1833	1.3736
30	12.0222	1.3018	8.5789	1.3670	8.2321	1.3736	8.1935	1.3744
40	11.3768	1.3145	8.5188	1.3687	8.2313	1.3742	8.1994	1.3748
50	10.9511	1.3229	8.4792	1.3698	8.2308	1.3746	8.2032	1.3751
60	10.6454	1.3290	8.4509	1.3706	8.2304	1.3749	8.2059	1.3753
70	10.4134	1.3336	8.4294	1.3713	8.2302	1.3751	8.2080	1.3755
80	10.2302	1.3372	8.4124	1.3717	8.2299	1.3752	8.2097	1.3756
90	10.0812	1.3401	8.3986	1.3721	8.2298	1.3754	8.2110	1.3757
100	9.9572	1.3426	8.3871	1.3725	8.2296	1.3755	8.2121	1.3758
$\varepsilon = \sqrt{10}$								
0.1	58.2948	0.5056	13.5153	1.1995	8.2553	1.3162	7.6602	1.3299
1	29.2320	0.9754	10.2414	1.3166	8.2496	1.3566	8.0272	1.3611
10	13.5364	1.2720	8.7204	1.3629	8.2339	1.3722	8.1798	1.3733
20	11.6264	1.3096	8.5420	1.3680	8.2316	1.3740	8.1971	1.3747
30	10.8383	1.3251	8.4688	1.3701	8.2307	1.3747	8.2042	1.3752
40	10.3906	1.3340	8.4273	1.3713	8.2301	1.3751	8.2082	1.3755
50	10.0960	1.3398	8.34	1.3721	8.2298	1.3754	8.2109	1.3757
60	9.8850	1.3440	8.3804	1.3727	8.2295	1.3755	8.2127	1.3759
70	9.7250	1.3472	8.3656	1.3731	8.2293	1.3757	8.2142	1.3760
80	9.5989	1.3497	8.3540	1.3734	8.2292	1.3758	8.2153	1.3761
90	9.4964	1.3517	8.3445	1.3737	8.2290	1.3759	8.2162	1.3761
100	9.4111	1.3534	8.3366	1.3739	8.2289	1.3760	8.2170	1.3762
$\varepsilon = 10$								
0.1	52.0066	0.5973	12.7288	1.2305	8.2585	1.3270	7.7548	1.3382
1	23.4961	1.0810	9.6726	1.3344	8.2445	1.3627	8.0853	1.3658
10	11.8951	1.3043	8.5671	1.3673	8.2319	1.3737	8.1947	1.3745
20	10.5635	1.3306	8.4433	1.3709	8.2303	1.3749	8.2067	1.3754
30	10.0181	1.3414	8.3928	1.3723	8.2297	1.3754	8.2116	1.3758
40	9.7093	1.3475	8.3642	1.3731	8.2293	1.3757	8.2143	1.3760
50	9.5066	1.3515	8.3454	1.3736	8.2291	1.3759	8.2161	1.3761
60	9.3615	1.3544	8.3320	1.3740	8.2289	1.3760	8.2174	1.3762
70	9.2516	1.3566	8.3219	1.3743	8.2287	1.3761	8.2184	1.3763
80	9.1650	1.3583	8.3139	1.3745	8.2286	1.3762	8.2192	1.3764
90	9.0947	1.3597	8.3074	1.3747	8.2285	1.3762	8.2198	1.3764
100	9.0363	1.3609	8.3020	1.3749	8.2285	1.3763	8.2203	1.3764

Table 7 Nusselt number and centerline temperature values for LPTT fluid flow in a constant wall temperature slit for positive Brinkman numbers at different values of extensibility parameter and Deborah number

De	Br = 0		Br = 0.1		Br = 1		Br = 10	
	Nu	T_c	Nu	T_c	Nu	T_c	Nu	T_c
$\epsilon = 1$								
0.1	7.5941	1.3239	6.9344	1.3396	0.8690	1.4893	-72.5868	3.9464
1	7.9512	1.3549	7.6473	1.3612	4.8924	1.4195	-24.6043	2.1366
10	8.1583	1.3716	8.0801	1.3731	7.3750	1.3869	0.2189	1.5318
20	8.1833	1.3736	8.1331	1.3745	7.6811	1.3833	3.1190	1.4737
30	8.1935	1.3744	8.1550	1.3751	7.8076	1.3818	4.3093	1.4505
40	8.1994	1.3748	8.1674	1.3754	7.8795	1.3810	4.9839	1.4376
50	8.2032	1.3751	8.1756	1.3757	7.9268	1.3804	5.4270	1.4291
60	8.2059	1.3753	8.1814	1.3758	7.9608	1.3801	5.7443	1.4231
70	8.2080	1.3755	8.1859	1.3759	7.9865	1.3798	5.9845	1.4186
80	8.2097	1.3756	8.1894	1.3760	8.0068	1.3795	6.1740	1.4150
90	8.2110	1.3757	8.1922	1.3761	8.0233	1.3793	6.3278	1.4121
100	8.2121	1.3758	8.1946	1.3762	8.0370	1.3792	6.4557	1.4098
$\epsilon = \sqrt{10}$								
0.1	7.6602	1.3299	7.0629	1.3437	1.5885	1.4748	-63.0771	3.5089
1	8.0272	1.3611	7.8047	1.3657	5.7916	1.4070	-15.3090	1.8861
10	8.1798	1.3733	8.1256	1.3743	7.6380	1.3838	2.7123	1.4817
20	8.1971	1.3747	8.1626	1.3753	7.8517	1.3813	4.7234	1.4426
30	8.2042	1.3752	8.1777	1.3757	7.9394	1.3803	5.5442	1.4269
40	8.2082	1.3755	8.1863	1.3759	7.9890	1.3797	6.0082	1.4182
50	8.2109	1.3757	8.1919	1.3761	8.0216	1.3794	6.3125	1.4124
60	8.2127	1.3759	8.1960	1.3762	8.0449	1.3791	6.5302	1.4084
70	8.2142	1.3760	8.1990	1.3763	8.0626	1.3789	6.6949	1.4053
80	8.2153	1.3761	8.2014	1.3763	8.0765	1.3787	6.8247	1.4029
90	8.2162	1.3761	8.2034	1.3764	8.0879	1.3786	6.93	1.4009
100	8.2170	1.3762	8.2050	1.3764	8.0973	1.3785	7.0176	1.3993
$\epsilon = 10$								
0.1	7.7548	1.3382	7.2497	1.3495	2.6388	1.4554	-49.9816	2.9783
1	8.0853	1.3658	7.9260	1.3690	6.4876	1.3979	-8.3664	1.7183
10	8.1947	1.3745	8.1574	1.3752	7.8218	1.3817	4.4424	1.4480
20	8.2067	1.3754	8.1830	1.3758	7.9698	1.3799	5.8291	1.4215
30	8.2116	1.3758	8.1934	1.3761	8.0302	1.3793	6.3929	1.4109
40	8.2143	1.3760	8.1993	1.3763	8.0644	1.3789	6.7111	1.4050
50	8.2161	1.3761	8.2032	1.3764	8.0867	1.3786	6.9195	1.4011
60	8.2174	1.3762	8.2059	1.3764	8.1027	1.3784	7.0685	1.3983
70	8.2184	1.3763	8.2080	1.3765	8.1148	1.3783	7.1812	1.3962
80	8.2192	1.3764	8.2097	1.3765	8.1244	1.3782	7.27	1.3946
90	8.2198	1.3764	8.2110	1.3766	8.1321	1.3781	7.3420	1.3933
100	8.2203	1.3764	8.2121	1.3766	8.1386	1.3780	7.4019	1.3922

Table 8 Nusselt number data as a function of εDe^2 in a slit flow for different values of Brinkman number

εDe^2	Br = -1	Br = -0.2	Br = 0	Br = 0.2	Br = 1
0.001	14.3941	8.9427	7.5474	6.1387	0.3682
0.01	14.0384	8.9049	7.5941	6.2719	0.8690
0.02	13.7592	8.8748	7.6297	6.3748	1.2554
0.03	13.5457	8.8516	7.6564	6.4525	1.5472
0.04	13.3728	8.8326	7.6777	6.5148	1.7814
0.05	13.2277	8.8166	7.6954	6.5668	1.9765
0.06	13.1029	8.8027	7.7105	6.6112	2.1435
0.07	12.9934	8.7905	7.7236	6.65	2.2892
0.08	12.8960	8.7796	7.7351	6.6844	2.4183
0.09	12.8084	8.7698	7.7455	6.7152	2.5340
0.1	12.7288	8.7609	7.7548	6.7431	2.6388
0.2	12.1877	8.6995	7.8172	6.9308	3.3436
0.3	11.8674	8.6627	7.8532	7.0403	3.7551
0.4	11.6430	8.6367	7.8780	7.1164	4.0410
0.5	11.4721	8.6169	7.8967	7.1740	4.2576
0.6	11.3352	8.6009	7.9116	7.2201	4.4305
0.7	11.2215	8.5876	7.9239	7.2581	4.5736
0.8	11.1247	8.5763	7.9343	7.2904	4.6950
0.9	11.0409	8.5665	7.9433	7.3183	4.8001
1.0	10.9670	8.5578	7.9512	7.3429	4.8924
2.0	10.5115	8.5039	7.9992	7.4933	5.4584
3.0	10.2712	8.4753	8.0242	7.5721	5.7550
4.0	10.1126	8.4564	8.0405	7.6238	5.9498
5.0	9.9965	8.4425	8.0524	7.6616	6.0921
6.0	9.9059	8.4316	8.0616	7.6910	6.2029
7.0	9.8324	8.4228	8.0691	7.7149	6.2927
8.0	9.7709	8.4154	8.0754	7.7348	6.3678
9.0	9.7183	8.4091	8.0807	7.7518	6.4319
10.0	9.6726	8.4036	8.0853	7.7666	6.4876
20.0	9.4010	8.3708	8.1126	7.8541	6.8174
30.0	9.2641	8.3542	8.1262	7.8980	6.9832
40.0	9.1759	8.3435	8.1350	7.9262	7.0897
50.0	9.1123	8.3358	8.1413	7.9466	7.1664
60.0	9.0634	8.3298	8.1461	7.9622	7.2255
70.0	9.0239	8.3250	8.15	7.9748	7.2731
80.0	8.9912	8.3210	8.1532	7.9853	7.3125
90.0	8.9633	8.3176	8.1559	7.9942	7.3460
100.0	8.9392	8.3147	8.1583	8.0019	7.3750

Table 9 Centerline temperature values as a function of εDe^2 in slit flow for different values of Brinkman number

εDe^2	Br = -1	Br = -0.2	Br = 0	Br = 0.2	Br = 1
0.001	1.1619	1.2864	1.3197	1.3539	1.5001
0.01	1.1776	1.2932	1.3239	1.3554	1.4893
0.02	1.1894	1.2983	1.3271	1.3566	1.4814
0.03	1.1983	1.3021	1.3295	1.3575	1.4756
0.04	1.2053	1.3051	1.3314	1.3582	1.4711
0.05	1.2111	1.3076	1.3330	1.3588	1.4674
0.06	1.2160	1.3097	1.3343	1.3594	1.4643
0.07	1.2203	1.3116	1.3355	1.3598	1.4616
0.08	1.2241	1.3132	1.3365	1.3602	1.4593
0.09	1.2274	1.3146	1.3374	1.3605	1.4572
0.1	1.2305	1.3159	1.3382	1.3609	1.4554
0.2	1.2506	1.3245	1.3436	1.3630	1.4434
0.3	1.2621	1.3293	1.3467	1.3642	1.4368
0.4	1.27	1.3326	1.3488	1.3651	1.4323
0.5	1.2759	1.3351	1.3503	1.3657	1.4289
0.6	1.2806	1.3371	1.3516	1.3662	1.4263
0.7	1.2845	1.3387	1.3526	1.3667	1.4242
0.8	1.2878	1.3401	1.3535	1.3670	1.4224
0.9	1.2906	1.3413	1.3542	1.3673	1.4209
1.0	1.2931	1.3423	1.3549	1.3676	1.4195
2.0	1.3080	1.3485	1.3588	1.3692	1.4116
3.0	1.3157	1.3517	1.3609	1.3701	1.4075
4.0	1.3207	1.3538	1.3622	1.3707	1.4049
5.0	1.3244	1.3553	1.3632	1.3711	1.4030
6.0	1.3272	1.3565	1.3639	1.3714	1.4016
7.0	1.3295	1.3574	1.3645	1.3716	1.4004
8.0	1.3314	1.3582	1.3650	1.3718	1.3994
9.0	1.3330	1.3589	1.3655	1.3720	1.3986
10.0	1.3344	1.3595	1.3658	1.3722	1.3979
20.0	1.3427	1.3629	1.3680	1.3731	1.3938
30.0	1.3468	1.3646	1.3691	1.3736	1.3917
40.0	1.3494	1.3657	1.3698	1.3739	1.3904
50.0	1.3513	1.3665	1.3703	1.3741	1.3895
60.0	1.3528	1.3671	1.3707	1.3743	1.3887
70.0	1.3540	1.3675	1.3710	1.3744	1.3882
80.0	1.3549	1.3679	1.3712	1.3745	1.3877
90.0	1.3557	1.3683	1.3714	1.3746	1.3873
100.0	1.3564	1.3686	1.3716	1.3747	1.3869

References

- Barletta A, di Schio ER, Zanchini E (2003) Combined forced and free flow in a vertical rectangular duct with prescribed wall heat flux. *Int J Heat Fluid Flow* 24:874–887
- Chang SW, Yang TL, Huang RF, Sung KC (2007) Influence of channel-height on heat transfer in rectangular channels with skewed ribs at different bleed conditions. *Int J Heat Mass Transf* 50:4581–4599
- Sayed-Ahmed M, Kishk KM (2008) Heat transfer for Herschel–Bulkley fluids in the entrance region of a rectangular duct. *Int Commun Heat Mass Transf* 35:1007–1016
- Norouzi M, Kayhani M, Nobari M (2009) Mixed and forced convection of viscoelastic materials in straight duct with rectangular cross section. *World Appl Sci J* 7:285–296
- Rao SS, Ramacharyulu NCP, Krishnamurthy V (1969) Laminar forced convection in elliptic ducts. *Appl Sci Res* 21:185–193
- Bhatti M (1984) Heat transfer in the fully developed region of elliptical ducts with uniform wall heat flux. *J Heat Transf* 106:895–898
- Abdel-Wahed R, Attia A, Hifni M (1984) Experiments on laminar flow and heat transfer in an elliptical duct. *Int J Heat Mass Transf* 27:2397–2413
- Sakalis V, Hatzikonstantinou P, Kafousias N (2002) Thermally developing flow in elliptic ducts with axially variable wall temperature distribution. *Int J Heat Mass Transf* 45:25–35
- Maia CRM, Aparecido JB, Milanez LF (2006) Heat transfer in laminar flow of non-Newtonian fluids in ducts of elliptical section. *Int J Therm Sci* 45:1066–1072
- Oliveira PJ, Pinho FT (1999) Analytical solution for fully developed channel and pipe flow of Phan–Thien–Tanner fluids. *J Fluid Mech* 387:271–280
- Pinho F, Oliveira P (2000) Analysis of forced convection in pipes and channels with the simplified Phan–Thien–Tanner fluid. *Int J Heat Mass Transf* 43:2273–2287
- Coelho P, Pinho F, Oliveira P (2002) Fully developed forced convection of the Phan–Thien–Tanner fluid in ducts with a constant wall temperature. *Int J Heat Mass Transf* 45:1413–1423
- Pinho F, Coelho P (2006) Fully-developed heat transfer in annuli for viscoelastic fluids with viscous dissipation. *J Nonnewton Fluid Mech* 138:7–21
- Norouzi M (2016) Analytical solution for the convection of Phan–Thien–Tanner fluids in isothermal pipes. *Int J Therm Sci* 108:165–173
- Anand V (2016) Effect of slip on heat transfer and entropy generation characteristics of simplified Phan–Thien–Tanner fluids with viscous dissipation under uniform heat flux boundary conditions: exponential formulation. *Appl Therm Eng* 98:455–473
- Matías A, Sánchez S, Méndez F, Bautista O (2015) Influence of slip wall effect on a non-isothermal electro-osmotic flow of a viscoelastic fluid. *Int J Therm Sci* 98:352–363
- Khan M, Hussain A, Malik M, Salahuddin T, Aly S (2019) Numerical analysis of Carreau fluid flow for generalized Fourier's and Fick's laws. *Appl Numer Math* 144:100–117
- Hussain A, Malik MY, Khan M, Salahuddin T (2019) Application of generalized Fourier heat conduction law on MHD viscoelastic fluid flow over stretching surface. *Int J Numer Methods Heat Fluid Flow*. <https://doi.org/10.1108/HFF-02-2019-0161>
- Khan M, Salahuddin T, Malik M, Khan F (2019) Arrhenius activation in MHD radiative Maxwell nanofluid flow along with transformed internal energy. *Eur Phys J Plus* 134:198
- Khan M, Malik M, Salahuddin T, Saleem S, Hussain A (2019) Change in viscosity of Maxwell fluid flow due to thermal and solutal stratifications. *J Mol Liq* 288:110970
- Salahuddin T, Muhammad S, Sakinder S (2019) Impact of generalized heat and mass flux models on Darcy–Forchheimer Williamson nanofluid flow with variable viscosity. *Phys Scr* 94:125201
- Khan M, Salahuddin T, Malik M (2019) Implementation of Darcy–Forchheimer effect on magnetohydrodynamic Carreau–Yasuda nanofluid flow: application of Von Kármán. *Can J Phys* 97:670–677
- Tanveer A, Salahuddin T (2019) Emission of electromagnetic waves from walls of esophagus under domination of wall slip effect. *Chaos Solitons Fractals* 127:110–117
- Salahuddin T, Tanveer A, Malik M (2019) Homogeneous-heterogeneous reaction effects in flow of tangent hyperbolic fluid on a stretching cylinder. *Can J Phys*. <https://doi.org/10.1139/cjp-2018-0552>
- Salahuddin T, Arif A, Haider A, Malik M (2018) Variable fluid properties of a second-grade fluid using two different temperature-dependent viscosity models. *J Braz Soc Mech Sci Eng* 40:575
- Haider A, Salahuddin T, Malik M (2018) Change in conductivity of magnetohydrodynamic Darcy–Forchheimer second grade fluid flow due to variable thickness surface. *Can J Phys* 97(8):809–815
- Cruz D, Pinho FTD, Oliveira P (2005) Analytical solutions for fully developed laminar flow of some viscoelastic liquids with a Newtonian solvent contribution. *J Non Newton Fluid Mech* 132:28–35
- Norouzi M, Daghighi S, Bég OA (2018) Exact analysis of heat convection of viscoelastic FENE-P fluids through isothermal slits and tubes. *Meccanica* 53:817–831
- Ou J-W, Cheng K (1974) Viscous dissipation effects on thermal entrance heat transfer in laminar and turbulent pipe flows with uniform wall temperature. In: *AIAA/ASME 1974 thermophysics and heat transfer conference*
- Basu T, Roy D (1985) Laminar heat transfer in a tube with viscous dissipation. *Int J Heat Mass Transf* 28:699–701
- Oliveira P, Coelho P, Pinho F (2004) The Graetz problem with viscous dissipation for FENE-P fluids. *J Non Newton Fluid Mech* 121:69–72
- Bejan A (2013) *Convection heat transfer*. Wiley, New York
- Thien NP, Tanner RI (1977) A new constitutive equation derived from network theory. *J Non Newton Fluid Mech* 2:353–365
- Peters GW, Baaijens FP (1997) Modelling of non-isothermal viscoelastic flows. *J Non Newton Fluid Mech* 68:205–224
- Eckert ERG, Drake RM Jr (1987) *Analysis of heat and mass transfer*. Tata McGraw Hill, New Delhi
- Nóbrega J, Pinho FTD, Oliveira P, Carneiro O (2004) Accounting for temperature-dependent properties in viscoelastic duct flows. *Int J Heat Mass Transf* 47:1141–1158
- Kays WM, Crawford ME, Weigand B (2012) *Convective heat and mass transfer*. Tata McGraw-Hill Education, New York

Publisher's Note Springer Nature remains neutral with regard to jurisdictional claims in published maps and institutional affiliations.